Journal of Medicinal Chemistry

ARTICLE

pubs.acs.org/jmc

Structure−Activity Relationship and Pharmacokinetic Studies of Sotrastaurin (AEB071), a Promising Novel Medicine for Prevention of Graft Rejection and Treatment of Psoriasis

Jürgen Wagner,* Peter von Matt,* Bernard Faller, Nigel G. Cooke, Rainer Albert, Richard Sedrani, Hansjörg Wiegand, Christian Jean, Christian Beerli, Gisbert Weckbecker, Jean-Pierre Evenou, Gerhard Zenke, and Sylvain Cottens

Novartis Institutes for BioMedical Research, Basel CH-4002, Switzerland

ABSTRACT: Protein kinase C (PKC) isotypes have emerged as key targets for the blockade of early T-cell activation. Herein, we report on the structure−activity relationship and the detailed physicochemical and in vivo pharmacokinetic properties of sotrastaurin (AEB071, **1**), a novel maleimide-based PKC inhibitor currently in phase II clinical trials. Most notably, the preferred uptake of sotrastaurin into lymphoid tissues is an important feature, which is likely to contribute to its in vivo efficacy.

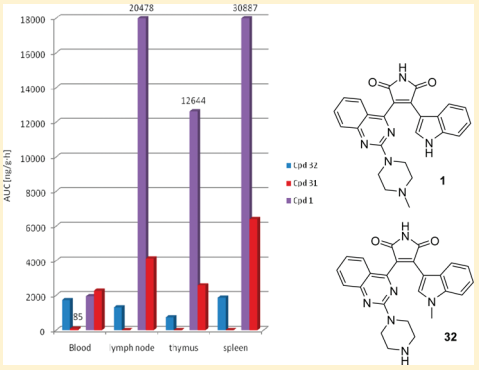

INTRODUCTION

Solid organ allotransplantation is currently the treatment of choice for patients with end stage renal, cardiac, hepatic, pancreatic, and pulmonary failure.[1−3] Despite the considerable impact on extending and improving the quality of life of patients, safer and better tolerated immunosuppressants are still an unmet medical need. In particular, the blockade of T-cell activation, which is a central event in the complex process of graft rejection, is currently only achieved in the clinical setting with calcineurin inhibitors like cyclosporine A (CsA) and tacrolimus. The therapeutic value of these agents, although widely used in transplant patients, is limited by mechanism-based side effects. Thus, novel and specific inhibitors of early T-cell activation acting though an alternative mechanism of action are of high interest. Recently, we reported preliminary results on the discovery of sotrastaurin (STN, AEB071, **1**), an immunosuppressant that inhibits classical and novel protein kinase C (PKC) isotypes.[4,5] The clinical data generated with **1** suggest that the pharmacologic inhibition of PKCs might offer an alternative mechanism-based therapeutic strategy for preventing early T-cell activation, thus providing unique treatment options for transplanted patients and patients suffering from T-cell dependent autoimmune pathologies like psoriasis.[6,7]

The PKC family of serine/threonine kinases plays a central role in signaling cascades of the immune system. The PKC isotypes are divided into three classes based on their cofactor requirements. Whereas the classical cPKCs α, β, and γ are regulated by diacylglycerol (DAG), phosphatidylserine (PS), and calcium, the novel nPKCs δ, ε, η, and θ require DAG and PS but are calcium insensitive. The atypical aPKCs ι/λ and ζ require neither DAG nor calcium.[8] In resting cells, the PKCs are predominantly localized in the cytosol and are catalytically inactive because of autoinhibition by their pseudosubstrate domain. Upon cell activation, PKC isotype-specific signals trigger translocation from the cytosol to the membrane and induce conformational changes, which displace the pseudosubstrate moiety from the catalytic domain and enable PKC isotypes to phosphorylate specific protein substrates. Interestingly, the unique function of each individual PKC isotype was only recently understood through the study of individual knockout mice.[9−11] On the basis of the analysis of such phenotypes, three PKC isotypes, namely, α, β, and θ, emerged as key regulators of T and B cell signaling pathways.

Herein, we report on the structure−activity relationship (SAR) around the quinazolinyl-indolyl-maleimide scaffold and describe in depth the in vitro and in vivo pharmacokinetic properties of **1**. In particular, the importance of tissue distribution into lymphatic organs is highlighted. Indeed, the striking difference in exposure between **1** and the structurally closely related analogue **32**, which is in contrast to **1** inefficacious in preclinical rat models, emphasizes the need to reach high drug levels in the main target organs.

SYNTHESIS

All quinazolinylindolyl derivatives were obtained from commercially available building blocks according to the synthesis

Received: April 19, 2011
Published: July 28, 2011

dx.doi.org/10.1021/jm200469u | *J. Med. Chem.* 2011, 54, 6028–6039

Scheme 1. Generic Synthesis of the Quinazolinyl Derivatives[a]

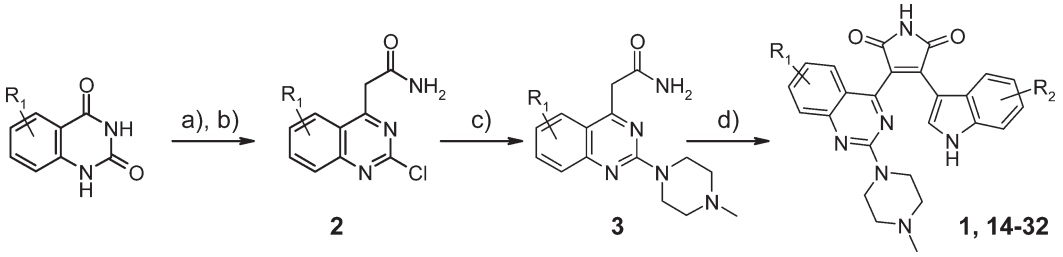

[a] Reagents and conditions: yields are given for **1** (R_1, R_2 = H); (a) $POCl_3$, dimethylphenylamine, 110 °C, 81%; (b) (i) 3-oxobutyric acid ethyl ester, NaH, THF, 0 °C, then toluene, 110 °C; (ii) NH_4OH, room temperature; (iii) ethyl acetate, 76 °C, 54%; (c) *N*-methylpiperazine, 1-methyl-2-pyrrolidinone, 50 °C, 69%; (d) (1*H*-indol-3-yl)oxoacetic acid methyl ester, KO^{t}Bu, THF, 0 °C to room temperature, 47%.

Scheme 2. Synthesis of the Naphthyl Derivative 7[a]

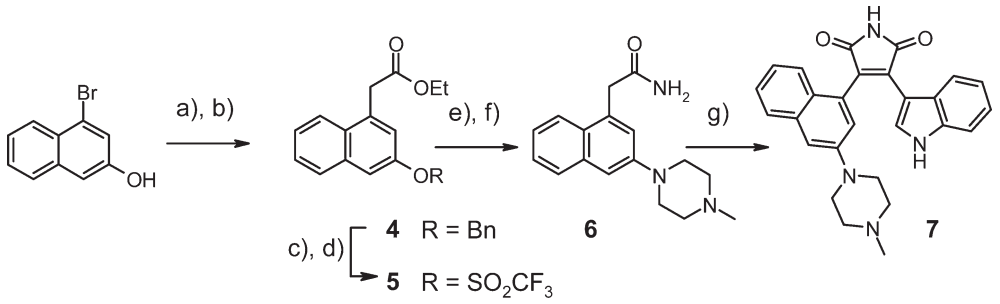

[a] Reagents and conditions: (a) NaH, BnBr, Bu_4NI (cat.), DMF, room temperature, 93%; (b) tributylstannanylacetic acid ethyl ester, $ZnBr_2$, $PdCl_2$-[P(*o*-tolyl)$_3$]$_2$ (0.2 equiv), DMF, 80 °C, 42%; (c) Pd/C 10%, H_2, MeOH, room temperature, 95%; (d) $(CF_3SO_2)_2O$, pyridine, CH_2Cl_2, room temperature, 89%; (e) $Pd_2(dba)_3$ (0.05 equiv), 2-(di-*tert*-butylphosphino)biphenyl (0.05 equiv), *N*-methylpiperazine, K_3PO_4, THF, 80 °C, 84%; (f) formamide, NaOMe, DMF, 105 °C, 92%; (g) (1*H*-indol-3-yl)oxoacetic acid methyl ester, KO^{t}Bu, THF, room temperature, 66%.

Scheme 3. Synthesis of the Quinolinyl Derivative 10[a]

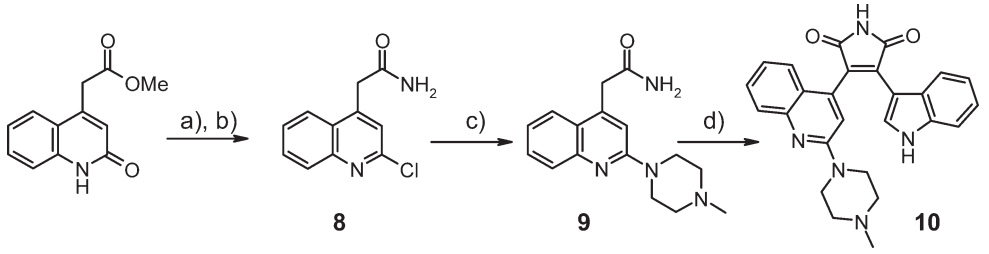

[a] Reagents and conditions: (a) $POCl_3$ (1.6 equiv), 2 h, 80 °C, 95%; (b) NH_4OH (28% aqueous), 16 h, room temperature, 62%; (c) *N*-methylpiperazine (5 equiv), NMP, 60 h, room temperature, 80%; (d) (1*H*-indol-3-yl)oxoacetic acid methyl ester (1 equiv), KO^{t}Bu (5 equiv), DMF, 19 h, 80 °C, 62%.

described for **1** in Scheme 1. The sodium salt of ethyl acetoacetate regioselectively replaced the 4-chloro atom of 2,4-dichloroquinazoline.[12] Upon exposure of the initially obtained adduct to aqueous ammonia, a retro-Claisen reaction and a primary amide formation ensued to afford **2**. Introduction of *N*-methylpiperazine resulted in intermediate **3** which was cyclized with (1*H*-indol-3-yl)oxoacetic acid methyl ester[13] under basic conditions to complete the synthesis of **1** in good yields.

Scheme 2 describes the synthesis of the naphthyl-based maleimide **7**. 4-Bromonaphthalen-2-ol was protected as the benzyl ether and submitted to a palladium-catalyzed coupling with preformed tributylstannanylacetic acid ethyl ester to form the intermediate ester **4**.[14] After hydrogenolytic removal of the benzyl group, the phenol was converted to the trifluoromethylsulfonate derivative **5**, which was used in the palladium-catalyzed coupling reaction with *N*-methylpiperazine.[15] Formamide in methanolic sodium methoxide served to directly convert the ester to the primary amide **6**,[16] which was used in the cyclocondensation reaction.

The synthesis of the quinolinyl derivative **10** is described in Scheme 3. The previously reported methyl ester[17] was converted into the 2-chloroquinolinyl intermediate, which was then stirred in aqueous ammonia to form the primary amide **8**. Room temperature coupling with *N*-methylpiperazine yielded **9**, which was used in the base-mediated cyclocondensation to afford maleimide **10**.

Finally, the synthesis of the isoquinolinyl-based maleimide **13** started from commercially available 1,3-dichloroisoquinoline (Scheme 4). The regioselective chlorine substitution with the sodium salt of malonic acid diethyl ester followed by in situ decarboxylation upon heating in xylene yielded the intermediate ester, which was converted to the primary amide **11** in methanolic ammonia. Cyclocondensation led to the intermediate

dx.doi.org/10.1021/jm200469u |*J. Med. Chem.* 2011, 54, 6028–6039

Scheme 4. Synthesis of the Isoquinolinyl Derivative 13[a]

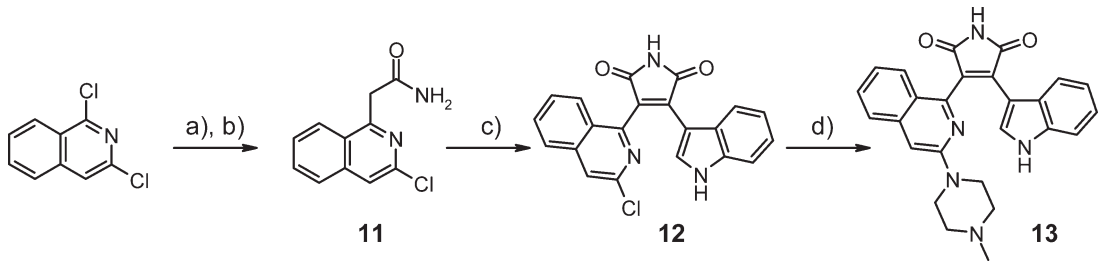

[a] Reagents and conditions: (a) malonic acid diethyl ester (3 equiv), NaH (2.8 equiv), xylene, 3 h, 140 °C, 62%; (b) NH_3 (4 M in MeOH), 16 h, 130 °C, 76%; (c) (1*H*-indol-3-yl)oxoacetic acid methyl ester (2.5 equiv), KO^{t}Bu (1 M in THF, 5 equiv), 1 h, 80 °C, 54%; (d) *N*-methylpiperazine, 18 h, 130 °C, 29%.

Table 1. Influence of Nitrogen Insertion on Isotype Selectivity

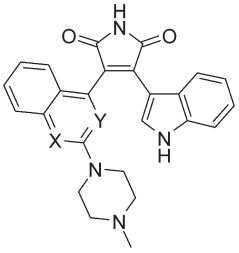

		PKC isotypes[a]						MLR[a,b]		TCR/CD28[a,c]
compd	X, Y	α	β_1	δ	ε	η	θ	mouse	human	Jurkat cells
1	N, N	2.1	2.0	1.3	6.2	6.1	1.0	150	37	54
7	C, C	0.9	1.8	7.3	19	25	4.8	123	25	50
10	N, C	3.6	5.2	27	72	118	31	575	nd	79
13	C, N	1.4	2.0	1.8	4.3	6.2	2.1	73	37	23

[a] IC_{50} values are reported in nM as the average of at least two independent experiments. [b] MLR = mixed lymphocyte reaction assay. nd = not determined. [c] Inhibition of IL-2 secretion after TCR/CD28-mediated activation of Jurkat cells.

Table 2. Influence of Substituents around the Quinazolinyl Moiety on Isotype Selectivity

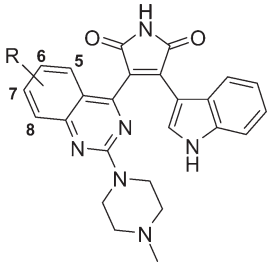

		PKC isotypes[a]					
compd	R	α	β_1	δ	ε	η	θ
14	5-Me	3.6	3.8	3.2	6.2	9.2	2.9
15	6-F	1.0	1.2	0.6	2.0	1.9	0.6
16	6-Cl	1.7	23	1.2	3.9	5.4	1.2
17	6-Me	7.5	140	4.1	16	25	5.1
18	6-^{i}Pr	>316	>316	12	>316	283	71
19	6-^{t}Bu	>316	>316	>316	>316	>316	>316
20	7-F	4.5	5.0	6.3	15.3	9.0	7.8
21	7-Cl	280	304	224	>316	192	316
22	8-Me	235	>316	52	334	197	67

[a] IC_{50} values are reported in nM as the average of at least two independent experiments.

maleimide **12**, which was transformed into the end product **13** through thermal substitution of chlorine with *N*-methylpiperazine.

RESULTS AND DISCUSSION

During the early stages of the chemical derivation program, our efforts focused on identifying the most promising bicyclic heteroaromatic moiety through modifications in positions X and Y (Table 1). The inhibitory potency on classical and novel PKC isotypes was determined by scintillation proximity assay (SPA) technology.[5] Results from these assays indicated that the replacement of the quinazolinyl by a naphthyl moiety in **7** reduced the potency by 5-fold on the novel PKC isotypes. In contrast, **7** retained full activity on the classical PKC isotypes α and β. Interestingly, the PKC activity of the quinolinyl derivative **10** was further reduced and single digit nanomolar potency was retained only on the classical isotypes. A very similar profile was measured for the partially hydrogenated 5,6,7,8-tetrahydronaphthyl derivative (data not shown), suggesting that the binding sites of PKC α and β are more flexible and can tolerate nonplanar fragments as well as polarity in position X of the quinazoline ring. These scaffolds may represent suitable leads for an approach aiming at specific inhibition of classical PKCs. Finally, the isoquinolinyl derivative **13** was equipotent to **1** on all isotypes, suggesting that the nitrogen atom in position X is not essential. Gratifyingly, the biochemical activity translated into prevention of T-cell activation measured by inhibition of IL-2 production after stimulation through the T cell receptor (TCR) and the coreceptor CD28.[5] Furthermore, the compounds also showed in vitro immunosuppressive activity as assessed in the mixed lymphocyte reaction (MLR) assay, which is a standard readout for alloantigen-induced T-cell proliferation.[5] The least potent derivative **10** was significantly less active in the mouse MLR, and as a general trend, the maleimides show superior inhibition of MLR responses using human rather than mouse cells. These derivatives are not general inhibitors of cell proliferation, as they affected the

Table 3. Influence of Substituents around the Indolyl Moiety on Isotype Selectivity

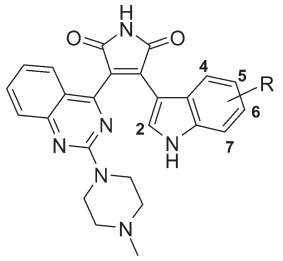

		PKC isotypes[a]					
compd	R	α	β_1	δ	ε	η	θ
23	4-Cl	202	48	93	>316	202	221
24	5-Cl	8.3	6.5	2.5	9.8	9.1	8.3
25	6-Cl	8.5	7.7	8.2	32	19	9.8
26	7-Cl	9.1	6.0	6.2	19	17	7.0
27	7-Me	0.4	0.2	0.1	0.7	1.7	0.1
28	*N*-Me	6.4	5.1	5.7	25	20	5.8
29	*N*-^{i}Pr	11	7.8	2.7	11	11	3.8
30	2-Me	63	22	25	73	65	26

[a] IC_{50} values are reported in nM as the average of at least two independent experiments.

proliferation of mouse bone marrow cells only in the micromolar range (IC_{50s} > 2.5 μM).[5] Further derivation efforts focused on the quinazolinyl scaffold because of the strong potency on PKC isotypes and the broad synthetic accessibility of the series.

In a second derivation round, the impact of substituents in positions 5−8 of the quinazolinyl fragment on potency and selectivity was explored (Table 2). Modifications in position 5 had little effect on activity as represented by the 5-methyl derivative **14**. In contrast, derivation of position 6 was more attractive, as it allowed modulation of the PKC isotype specificity. The 6-fluoro analogue **15** is the most potent derivative of the series and marginally superior over **1**. By increasing the bulk of the substituent, the activity on PKC β is gradually lost. This is well demonstrated by the chloro and methyl analogues **16** and **17**. The hydrophobic cavity was further explored with the isopropyl analogue **18**, which is inactive on all assayed isotypes except PKC δ and θ. These two PKC isotypes are phylogenetically most closely related and the comparable inhibitory activity is thus not unexpected.[8] Finally, all PKC activity is lost with the *tert*-butyl analogue **19**. Our attempts to substitute positions 7 and 8 were unsuccessful, as the activity on the target was rapidly lost with derivatives **20**−**22**. Even the 7-fluoro analogue **20**, with the sterically least demanding group, showed reduced potency. These results are confirmed by the X-ray crystal structure of **1** bound to the ATP-binding site of PKC α.[4] Indeed, the structure suggests that substituents in this part of the quinazolinyl moiety would clash with several residues of the protein in spatial proximity including Val_{353}, Lys_{368}, Met_{417}, and Phe_{350}. Overall, these results show that modifying position 6 of the quinazolinyl fragment has a strong impact on the PKC selectivity profile. Consequently, further derivation thereof may well lead to the identification of tool compounds with unique specificities and therefore of high value to test the role of individual isotypes in cellular signaling pathways.

Table 4. Physicochemical Characteristics of 1 in Comparison to 32[a]

parameter	1	32
MW	438.49	438.49
PSA	94	94
pK_a	9.3/7.5/2.4	9.5/8.4/2.0
log *P*	2.9	2.3
$\log D_{pH6.8}$	2.4	0.6
$Sol_{pH6.8}$ (g/L)	0.019	0.195
$SGF_{pH2.0}$ (g/L)[b]	0.78	nd
$FaSSIF_{pH6.5}$ (g/L)[c]	0.41	nd
$FeSSIF_{pH5.8}$ (g/L)[d]	0.53	nd
logPAMPA (cm/s)[e]	−5.3	−5.2
Caco-2 $(B-A_{pp})^f/(A-B_{pp})^g$	1.37	nd
MDCK1 $(B\text{-}A_{pp})^f/(A-B_{pp})^g$	43	64.4

[a] nd = not determined. [b] SGF: solubility in simulated gastric fluid. [c] FaSSIF: solubility in simulated intestinal fluid (fasted state). [d] FeSSIF: solubility in simulated intestinal fluid (fed state). [e] logPAMPA: permeability measured in a PAMPA assay. [f] $B-A_{pp}$: basal to apical permeability. [g] $A-B_{pp}$: apical to basolateral permeability.

As reported previously, attempts to identify replacements for the unsubstituted indolyl fragment attached to the maleimide were unsuccessful.[4] However, the introduction of a series of modifications on the periphery of the indolyl fragment was more rewarding (Table 3). An initial fluorine scan in positions 4−7 of the indolyl had negligible effects on potency (data not shown). A similar screen with a bulky hydrophobic group like chlorine revealed a very similar PKC profile for the 5-, 6-, and 7-chlorine derivatives **24**−**26** with moderate activity retained on all isotypes. In contrast, the 4-chlorine analogue **23** was mostly inactive. Further derivation of position 7 resulted in the methyl analogue **27**, which shows subnanomolar potency on all classical and novel PKC isotypes and is one of the most potent PKC inhibitor reported so far. Finally, the modest effect on enzymatic activity of the *N*-methyl and *N*-isopropyl analogues **28** and **29** suggests that large hydrophobic side chains attached to the indole nitrogen are tolerated. On the other hand, the 2-methyl derivative **30** lost 10- to 30-fold in activity. Reduced rotational freedom of **30** may account for or contribute to the loss of activity. In conclusion, the derivation efforts around the indolyl group suggested that substituents are tolerated in several positions around the indolyl moiety but did not result in superior derivatives except for **27**. Unfortunately, **27** could not be further considered for development because the stronger activity in mouse and human MLR, 77 and 15 nM, respectively, was offset by the low bioavailability and higher clearance in single dose rat pharmacokinetic studies (data not shown).

The excellent enzymatic and cellular profile prompted us to consider **1** for further development. Its in vitro physicochemical characteristics are summarized in Table 4. **1** is a maleimide derivative with a weakly basic piperazine moiety (pK_a = 7.4) resulting in a fraction ionized of 0.8 under physiological pH. Its moderate intrinsic solubility at pH 6.8 is clearly below what is anticipated from its log *P*, suggesting that factors other than lipophilicity hinder solubility. In both fasted state simulated intestinal fluid (FaSSIF) and fed state simulated intestinal fluid (FeSSIF), the solubility was good. **1** showed moderate membrane permeability as measured in the parallel artificial membrane permeation assay (PAMPA) and confirmed using the

Table 5. Pharmacokinetic Properties of 1 and 32 in Mouse, Rat, and Cynomolgus Monkeys

	1			32
parameter	mouse	rat	cynomolgus monkey	rat
iv dose (mg/kg)[a]	5	5	5	5
$AUC_{0-\infty}$ (ng·h/mL)[b]	371	326	720	671
Cl ((mL/min)/kg)[c]	45	51	23	25
V_{ss} (L/kg)[d]	3.1	6.5	5.9	10
$T_{1/2}$ (h)[e]	2.5	3.2	4.8	4.6
po dose (mg/kg)[f]	30	20	20	20
$AUC_{0-\infty}$ (ng·h/mL)[b]	72	110	128	161
T_{max} (h)	0.5	0.5	8.0	0.5
F (%)[g]	19	34	18	24
in vitro Cl_{int} ((μL/min)/mg)	248	505	433	112
PPB (% unbound)	nd	1.1− 3.1	2.4− 4.7	nd

[a] iv formulations are as follows. Balb/c mouse: PEG200/glucose. OFA rat: 80% saline (0.9%)/20% PEG400. Monkey: PEG400/0.1 M HCl/glucose. [b] Area under the curve extrapolated to infinity, dose normalized. [c] Total plasma clearance. [d] Volume of distribution. [e] Elimination half-life. [f] po formulations are as follows. Balb/c mouse: PEG200/glucose. OFA rat: 80% water/20% PEG400. Monkey: PEG400/0.1 M HCl/water. [g] Oral bioavailability. For **32**, 20% PEG400/glucose/0.1 M HCl was used for iv and po administration. Data reported as average of three animals.

Table 6. Potency on PKC Isotypes of the Active Metabolite and Close Analogues of 1

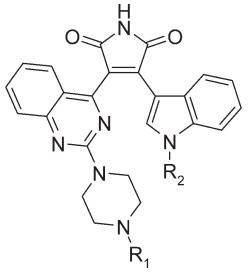

		PKC isotypes[a]						MLR[a,b]	
compd	R_1, R_2	α	β_1	δ	ε	η	θ	mouse	human
31	H, H	0.5	0.6	0.4	0.9	1.0	0.5	854	51
32	H, Me	1.4	1.4	1.0	3.8	3.3	1.2	378	99

[a] IC_{50} values are reported in nM as the average of at least two independent experiments. [b] MLR = mixed lymphocyte reaction assay.

human colon carcinoma epithelial cell line Caco-2 (P_{app} = 4.5 × 10^{-6} cm/s). The strong difference in efflux ratio measured with Caco-2 or Madin−Darby canine kidney (MDCK) cells, stably transfected with the gene for human p-glycoprotein, strongly suggested that **1** is a substrate for Pgp. Consequently, it is not surprising that **1** does not cross the blood−brain barrier. In vivo pharmacokinetic studies in mice, rats, and cynomolgus monkeys (Table 5) revealed that **1** had in all species a medium clearance, which was clearly below the rates expected from the in vitro data using liver microsomes. The difference may be explained by the modest transcellular permeability of this molecule, preventing a

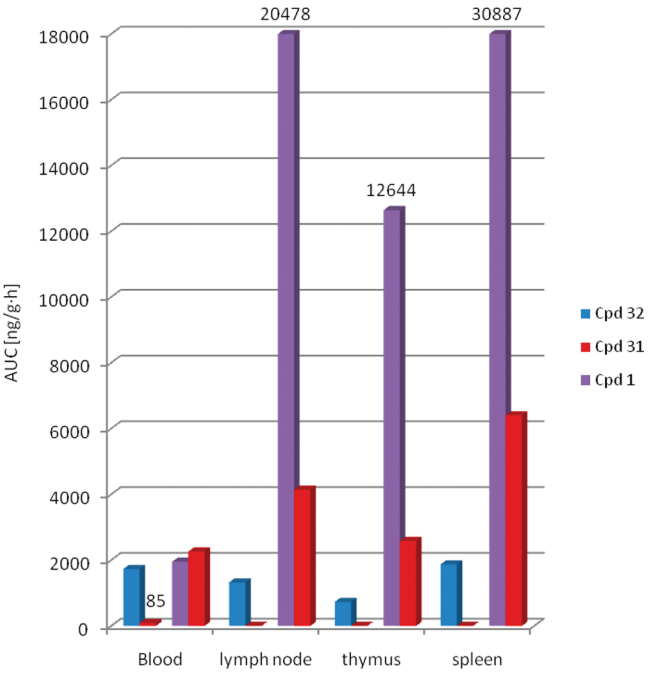

Figure 1. Area under concentration time curve in blood, mesenteric lymph node, spleen, thymus after peroral administration of 30 mg/kg **1** or **32** to male Wistar rats. In situ formation of metabolite **31** was measured in parallel after administration of either **1** or **32**. Formulation was PEG400/1 M HCl/5% glucose.

quick uptake by hepatocytes. The high plasma protein binding might be another factor influencing the in vivo clearance. Exposure of **1** in monkeys is prolonged in comparison to rodents because of a later T_{max} and longer elimination half-life. **1** undergoes extensive metabolism through CYP3A4, and the metabolites are primarily excreted through the feces. The desmethylpiperazine derivative **31** is a major metabolite (Table 6), and the amounts formed after oral dosing are highly species dependent. In rats, the exposure of the metabolite is comparable or higher (2-fold) than of the parent, while in cynomolgus monkeys the metabolite represents only 8%, and in humans the percentage drops to 1.2% after a single dose.[18] **31** is an active metabolite that retains subnanomolar activity on all PKC isotypes assayed (Table 6). Unexpectedly and in contrast to **1**, its immunosuppressive activity in the mouse but not human MLR is weak. Finally, **1** is also an inhibitor of CYP3A4-catalyzed midazolam 1′-hydroxylation in human liver microsomes with a K_i of 2.9 μM. To test the risk in exposure variation in the presence of a co-medication, a drug−drug interaction study was conducted in the clinic with ketoconazole as a strong CYP3A4 inhibitor.[18] Ketoconazole caused a 2.5-fold increase in maximum concentration and a 4.6-fold increase in the area under the curve of **1**, which is comparable to what is observed for other immunosuppressants like CsA.[19]

The lymphoid tissues, including lymph nodes, spleen, and thymus, are relevant target organs for drugs acting on the immune system. Therefore, we conducted a study in rats to compare the exposure of **1** in blood versus lymphoid tissues after oral administration. The structurally close analogue **32** was included into the study with the aim to understand striking differences in in vivo efficacies. Indeed, **32** was inefficacious in the rat heart allograft survival model at an oral dose of 30 mg/kg b.i.d. which was fully efficacious for **1**[20] despite very similar

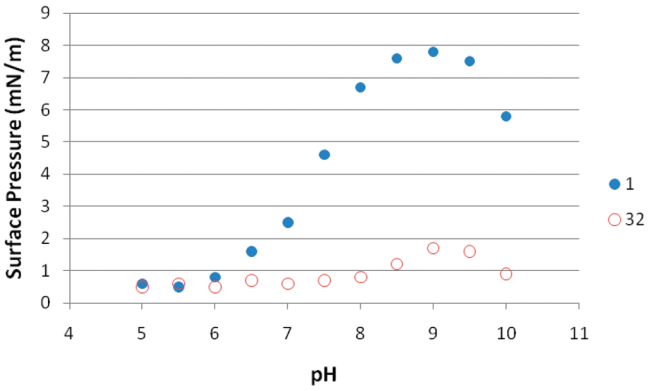

Figure 2. Surface activity pH profiles of **1** and **32**.

activity in the biochemical assays as well as in terms of physicochemical and pharmacokinetic properties (see Tables 4−6). The exposures measured in Wistar rats after a single oral dose of 30 mg/kg **1** or **32** are summarized in Figure 1. As expected from the initial PK studies, the areas under the curve in circulation for both compounds are very comparable (AUC_{0-24h} of 1952 and 1729 [ng/(g·h)] for **1** and **32**, respectively). However, important differences were observed in exposures in the lymphoid tissues. **1** reached up to 16-fold higher levels in the target organs, while the exposure of **32** was comparable in both blood and lymphoid tissues. This large difference cannot be accounted for by volume of distribution only. The study also confirmed that the active metabolite **31** was formed in high amounts in rats after oral dosing of **1**. On the other hand, only negligible levels of **31** were measured after administration of **32**. These results suggest that two factors may contribute to the superior in vivo efficacy of **1**. The high drug levels in the disease-specific target organs are critical to achieve the strong pharmacodynamic effect, which may be further enhanced by the contribution of the active metabolite **31**. Unfortunately, the underlying reasons explaining the different tissue distribution of the two molecules are poorly understood, and only a hypothesis can be offered herein. Derivatives **1** and **32** differ only marginally in terms of physicochemical properties: the log $D_{pH6.8}$ of **1** is higher because of the shift in the piperazine pK_a upon methylation, and the surface activity pH profiles[21] of **1** and **32** are fairly different (Figure 2). The amphiphilic nature of **1** was not anticipated from its 2D chemical structure and is uncovered upon deprotonation of the piperazine moiety, suggesting a 3D rearrangement of the molecule. The tendency of the molecule to form micelles suggests that **1** could form mixed micelles with bile salts and be absorbed to some extent via the lymphatic system, mimicking the absorption of dietary fats.[22−24] Contribution of the intestinal lymphatics to the overall absorption has been postulated for compounds including halofantrine, CsA, probucol, mepitiostane.[24]

CONCLUSIONS

In summary, sotrastaurin (**1**) is a potent and selective inhibitor of classical and novel PKC isotypes efficacious in rodent transplant models.[20] The detailed structure−activity relationship studies around the quinazolinyl and indolyl moieties confirmed the tight fit of the maleimide derivative into the ATP binding site of protein kinase C isotypes. Furthermore, isotype specific derivatives were identified through modifications in position 6 of the quinazolinyl fragment. The special pharmacokinetic properties of **1**, like the selective uptake into lymphoid tissues, are likely to contribute to its strong pharmacodynamic effects in rodent preclinical models. On this basis, **1** is currently tested as monotherapy in patients with psoriasis and as part of a regimen in combination with other immunosuppressants for prevention of kidney transplant rejection. These phase II clinical trials are underway to explore the clinical potential of sotrastaurin (**1**) for patients suffering from T-cell dependent autoimmune diseases.

EXPERIMENTAL SECTION

General. All nonaqueous reactions were carried out under an inert gas atmosphere (nitrogen or argon) at room temperature, unless otherwise noted. Commercial reagents and anhydrous solvents were used without further purification. Analytical thin layer chromatography (TLC) and flash chromatography were performed on Merck silica gel 60 (230−400 mesh). Proton nuclear magnetic spectroscopy spectra were obtained on Bruker DPX400 and DRX500 instrumentation. Chemical shifts are reported in parts per million relative to Me_4Si as internal standard. Conventional abbreviations used for signal shape are as follows: s, singlet; d, doublet; dd, doublet of doublets; t, triplet; m, multiplet; br, broad. Mass spectrometry (MS) analyses were performed on a Micromass platform electrospray mass spectrometer, using positive and negative ionization. New final SAR compounds were determined to be consistent with proposed structures by ^1H and ^{13}C NMR, MS or HRMS, and IR and were greater than 95% pure as determined by reversed phase UPLC (Waters Acquity Ultra Performance LC; column, Acquity UPLC HSS T3 1.8 μm, 2.1 mm × 50 mm; UV detection, Waters Acquity Ultra Performance LC PDA detector; flow rate, 0.5 mL/min; solvent A, water with 0.1% trifluoroacetic acid; solvent B, acetonitrile with 0.1% trifluoroacetic acid; gradient, solvent B from 20% to 100%).

2-(2-Chloroquinazolin-4-yl)acetamide (2). To a suspension of 1*H*,3*H*-quinazoline-2,4-dione (10.0 g, 61.7 mmol) in $POCl_3$ (37 mL) was added dropwise *N*,*N*-dimethylaniline (7.8 mL, 1.0 equiv). The mixture was heated to 110 °C and kept at reflux for 3 h. The solution was cooled to room temperature and poured onto an ice−water mixture. The precipitate was filtered off and washed with H_2O. The solid was dissolved in ethyl acetate and washed with H_2O and brine. The organic layer was dried over Na_2SO_4 and evaporated to afford crude 2,4-dichloroquinazoline (10.0 g, 81%), which can be crystallized from toluene/pentane. EI-MS: 198 $[M - H]^-$, 163 $[M - Cl]^-$. Ethyl acetoacetate (5.1 mL, 2.0 equiv) dissolved in THF (25 mL) was added dropwise to a suspension of NaH (60%, 1.0 g, 1.3 equiv) in THF (25 mL) at 0 °C. The solution was stirred for 30 min at 0 °C, and the solvent was evaporated. The residue was dissolved in toluene (125 mL), and 2,4-dichloroquinazoline (4.0 g, 20.0 mmol) was added. The mixture was stirred for 30 min at reflux, cooled to room temperature, and concentrated. The oily residue was dissolved in aqueous NH_4OH, 25% (80 mL), and stirred overnight at room temperature. All volatile materials were evaporated, and the residue was taken up in ethyl acetate (80 mL). The suspension was heated at reflux for 15 min, cooled to 0 °C, and filtered to afford **2** (2.37 g, 54%) as a white solid. EI-MS: 220 $[M - H]^-$, 178. ^1H NMR (DMSO-d_6, 400 MHz): δ 4.21 (s, 2H), 7.24 (br s, 1H), 7.75−7.84 (m, 2H), 7.97 (d, J = 8.4 Hz, 1H), 8.08 (dd, J = 8.4, 7.5 Hz, 1H), 8.34 (d, J = 8.4 Hz, 1H). ^{13}C NMR (DMSO-d_6, 100.6 MHz): δ 42.2, 123.3, 127.0, 127.6, 128.7, 135.9, 151.6, 156.0, 169.7, 171.1. IR (KBr) ν_{max} 3299, 3135, 1681, 1546, 1388, 1286, 1196, 948, 770 cm^{-1}.

3-(1*H*-Indol-3-yl)-4-[2-(4-methylpiperazin-1-yl)quinazolin-4-yl]pyrrole-2,5-dione (1). **2** (220 mg, 1.0 mmol) was dissolved in 1-methyl-2-pyrrolidinone (2.0 mL), and *N*-methylpiperazine (555 μL, 5.0 equiv) was added. The mixture was heated for 45 min at 50 °C. Ethyl acetate was added, and the suspension was filtered to afford 2-[2-(4-methylpiperazin-1-yl)quinazolin-4-yl]acetamide (197 mg, 69%) as a white solid. ESI-MS: 308 $[M + Na]^+$, 286 $[M + H]^+$. ^1H NMR

(DMSO-d_6, 400 MHz): δ 2.24 (s, 3H), 2.40 (m, 4H), 3.86 (m, 4H), 3.98 (s, 2H), 7.12 (br s, 1H), 7.24 (dd, J = 8.2, 7.5 Hz, 1H), 7.49 (d, J = 8.4 Hz, 1H), 7.63−7.72 (m, 2H), 7.95 (d, J = 8.2 Hz, 1H). ^{13}C NMR (DMSO-d_6, 100.6 MHz): δ 42.6, 43.7, 46.1, 54.8, 119.0, 122.6, 125.9, 126.3, 134.2, 152.1, 158.2, 167.4, 170.4. IR (KBr) ν_{max} 3344, 3130, 2786, 1671, 1618, 1587, 1557, 1299, 1006, 751 cm^{-1}. 2-[2-(4-Methylpiperazin-1-yl)quinazolin-4-yl]acetamide (213 mg, 0.75 mmol) and 3-indoleglyoxylic acid methyl ester (167 mg, 1.1 equiv) were suspended in THF (15 mL). To the suspension was added dropwise at 0 °C KO^{t}Bu (1.0 M in THF, 2.25 mL, 3.0 equiv). The mixture was stirred at room temperature overnight. A second portion of glyoxalate (30 mg, 0.2 equiv) and KO^{t}Bu (0.5 mL) were added, and the mixture was stirred at room temperature for 24 h. Ethyl acetate was added, and the organic phase was washed with 1.0 M aqueous $NaHCO_3$ and brine. The organic layer was dried over Na_2SO_4 and evaporated. The residue was purified by flash chromatography (Et_2O/MeOH/aqueous NH_4OH 90:10:1) to afford **1** (155 mg, 47%) as an orange-red powder. ESI-MS: 437 $[M - H]^-$. HRMS: calcd for $C_{25}H_{22}N_6O_2$ $[M + H]^+$ 439.1882, found 439.1886. ^{1}H NMR (DMSO-d_6, 400 MHz): δ 2.13 (s, 3H), 2.16 (m, 4H), 3.69 (m, 4H), 6.35 (d, J = 8.0 Hz, 1H), 6.64 (dd, J = 7.8, 7.4 Hz, 1H), 7.02 (dd, J = 7.6, 7.4 Hz, 1H), 7.10 (dd, J = 7.8, 7.2 Hz, 1H), 7.38 (d, J = 8.2 Hz, 1H), 7.53 (d, J = 8.4 Hz, 1H), 7.63−7.73 (m, 2H), 8.13 (s, 1H), 11.29 (br s, 1H), 12.01 (br s, 1H). ^{13}C NMR (DMSO-d_6, 100.6 MHz): δ 43.9, 46.1, 54.5, 105.3, 112.8, 118.7, 120.4, 120.8, 122.8, 124.7, 125.1, 125.9, 127.3, 127.4, 133.1, 134.9, 136.9, 138.3, 152.7, 158.3, 162.5, 171.8, 172.1. IR (KBr) ν_{max} 3320, 2930, 1709, 1548, 1339, 1004, 745 cm^{-1}.

(3-Benzyloxynaphthalen-1-yl)acetic Acid Ethyl Ester (4). 4-Bromonaphthalen-2-ol (5.0 g, 22.4 mmol) was dissolved in dry DMF (50 mL) under an atmosphere of argon. Sodium hydride (986 mg of a 60% suspension in mineral oil, 592 mg, 24.7 mmol) was added, and the mixture was stirred at 50 °C for 1 h. After the mixture was cooled to room temperature, benzyl bromide (3.5 mL, 5.0 g, 29.1 mmol) and tetrabutylammonium iodide (828 mg, 2.24 mmol) were added. After 16 h at room temperature, the reaction mixture was diluted with ethyl acetate. The solution was washed twice with semiconcentrated brine. The combined organic layers were dried over Na_2SO_4, concentrated, and the residue was purified by flash chromatography (hexane/ethyl acetate, 100:0 to 95:5 to 90:10) to yield 3-benzyloxy-1-bromonaphthalene (6.50 g, 93%). ES-MS: 312 $[M + H]^+$. ^{1}H NMR ($CDCl_3$, 400 MHz) δ 5.22 (s, 2H), 7.25 (d, J = 1.5 Hz, 1H), 7.45 (m, 7H), 7.64 (d, J = 2.4 Hz, 1H), 7.75 (d, J = 7.8 Hz, 1H), 8.17 (d, J = 7.8 Hz, 1H). 3-Benzyloxy-1-bromonaphthalene (5.64 g, 18.0 mmol) was dissolved under an atmosphere of argon in dry DMF (100 mL). Tributylstannanylacetic acid ethyl ester (7.5 g, 19.8 mmol) was added, as well as [bis(tri-*o*-tolylphosphine)]palladium(II) dichloride (2.83 g, 3.6 mmol) and zinc(II) bromide (5.27 g, 23.4 mmol). The reaction mixture was heated to 80 °C for 3 h, cooled to room temperature, diluted with ethyl acetate, and washed twice with diluted brine. The combined organic layers were dried over Na_2SO_4. The solvent was removed, and the residue was purified by flash chromatography (hexane/ethyl acetate 100:0 to 97.5:2.5 to 95:5 to 90:10). The resulting oil, still containing tin residues, was stirred in a 1:1 mixture of ethyl acetate/1 M NaOH (200 mL) for 1 h. The mixture was extracted twice with ethyl acetate. The combined organic layers were washed twice with H_2O, dried over Na_2SO_4, and concentrated. The residue was purified by flash chromatography (hexane/ethyl acetate, 100:0 to 97:3 to 95:5 to 93:7 to 92:8 to 90:10) to yield **4** (2.43 g, 42%). ES-MS: 320 $[M + H]^+$. ^{1}H NMR (DMSO-d_6, 400 MHz) δ 1.18 (t, J = 7.2 Hz, 3H), 4.10 (q, J = 7.2 Hz, 2H), 4.11 (s, 2H), 5.25 (s, 2H), 7.21 (d, J = 3.0 Hz, 1H), 7.41 (m, 8H), 7.53 (d, J = 6.6 Hz, 1H), 7.84 (dd, J = 7.2 Hz, 1H).

(3-Trifluoromethanesulfonyloxynaphthalen-1-yl)acetic Acid Ethyl Ester (5). **4** (2.43 g, 7.6 mmol) was dissolved in MeOH (50 mL). Then 10% palladium on charcoal (807 mg) was added, and the reaction mixture was stirred at room temperature under an atmosphere of hydrogen (1 atm) for 14 h. The reaction mixture was filtered. Concentration yielded (3-hydroxynaphthalen-1-yl)acetic acid ethyl ester (1.67 g, 95%) of adequate purity for the next reaction step. ES-MS: 230 $[M + H]^+$. ^{1}H NMR (DMSO-d_6, 400 MHz) δ 1.18 (t, J = 7.2 Hz, 3H), 4.05 (s, 2H), 4.10 (q, J = 7.2 Hz, 2H), 7.04 (d, J = 1.8 Hz, 1H), 7.06 (d, J = 1.8 Hz, 1H), 7.30 (t, J = 7.8 Hz, 1H), 7.40 (t, J = 7.8 Hz, 1H), 7.70 (d, J = 7.8 Hz, 1H), 7.80 (d, J = 7.8 Hz, 1H). (3-Hydroxynaphthalen-1-yl)acetic acid ethyl ester (1.67 g, 7.25 mmol) was dissolved in CH_2Cl_2 (20 mL) under an atmosphere of argon. Pyridine (1.17 mL, 1.15 g, 14.5 mmol) was added, and the reaction mixture was cooled to 0 °C, whereupon trifluoromethanesulfonic anhydride (1.79 mL, 3.07 g, 10.9 mmol) was added dropwise. The reaction mixture was warmed to room temperature, and after 1 h at room temperature, TLC analysis indicated complete consumption of starting material. The reaction mixture was diluted with ethyl acetate and washed twice with H_2O. The combined organic layers were dried over Na_2SO_4, the solvent was removed, and the residue was purified by flash chromatography (hexanes/ethyl acetate, 100:0 to 97:3 to 95:5 to 93:7 to 90:10) to yield **5** (2.33 g, 89%). ES-MS: 362 $[M + H]^+$. ^{1}H NMR (DMSO-d_6, 400 MHz) δ 1.19 (t, J = 7.2 Hz, 3H), 4.11 (q, J = 7.2 Hz, 2H), 4.38 (s, 2H), 7.60 (d, J = 3.0 Hz, 1H), 7.70 (m, 2H), 8.03 (m, 1H), 8.12 (m, 2H).

2-[3-(4-Methylpiperazin-1-yl)naphthalen-1-yl]acetamide (6). **5** (500 mg, 1.4 mmol) and *N*-methylpiperazine (166 mg, 1.66 mmol) were dissolved in THF (10 mL). Potassium phosphate (410 mg, 1.93 mmol), $Pd_2(dba)_3$ (62 mg, 0.069 mmol), and biphenyl-2-yldi-*tert*-butylphosphane (21 mg, 0.064 mmol) were added. The reaction mixture was heated to 80 °C for 4 h. After the mixture was cooled to room temperature, filtered, and concentrated, the crude product was purified by flash chromatography (CH_2Cl_2/MeOH, 98:2 to 80:20) to afford the piperazine intermediate (360 mg, 84%) as an oil. ES-MS: 313 $[M + H]^+$, 335 $[M + H]^+$. ^{1}H NMR (DMSO-d_6, 400 MHz): δ 1.18 (t, J = 7.4 Hz, 3H), 2.25 (s, 3H), 2.48−2.54 (m, 4H), 3.23−3.28 (m, 4H), 4.06 (s, 2H), 4.09 (q, J = 7.4 Hz, 2H), 7.10 (d, J = 2.1 Hz, 1H), 7.28 (t, J = 8.4 Hz, 1H), 7.35 (d, J = 2.1 Hz, 1H), 7.39 (t, J = 8.4 Hz, 1H), 7.72−7.78 (m, 2H). The piperazine intermediate from the above reaction (355 mg, 1.14 mmol) and formamide (171 mg, 3.8 mmol) was dissolved in DMF (5 mL). The solution was heated to 105 °C, and a solution of sodium methoxide (5.4 M in MeOH, 148 μL) was slowly added over 15 min. After 1 h at 105 °C, an additional portion of sodium methoxide (63 μL) was added, and heating was continued for another hour. The reaction mixture was cooled to room temperature, diluted with water, and extracted sequentially with ethyl acetate and with CH_2Cl_2. The combined organic layers were dried over Na_2SO_4, filtered, and concentrated. Purification by flash chromatography (ethyl acetate/AcOH/H_2O, 700:110:90 to 650:130:120) afforded **6** (monoacetate, 358 mg, 92%) as a solid. ES-MS: 284 $[M + H]^+$, 306 $[M + Na]^+$. HRMS: calcd for $C_{17}H_{22}N_3O$ $[M + H]^+$ 284.175 74, found 284.175 84. ^{1}H NMR (DMSO-d_6, 500 MHz, trifluoroacetate salt): δ 2.88 (s, 3H), 3.01−3.12 (m, 2H), 3.16−3.27 (br, 2H), 3.53−3.63 (br, 2H), 3.81 (s, 2H), 3.91−4.01 (br, 2H), 6.97 (s, 1H), 7.19 (s, 1H), 7.33 (dd, J = 8.4, 7.4 Hz, 1H), 7.34 (s, 1H), 7.42 (dd, J = 8.2, 7.4 Hz, 1H), 7.54 (s, 1H), 7.75 (d, J = 8.2 Hz, 1H), 7.93 (d, J = 8.4 Hz, 1H), 10.08−10.20 (br, 1H). ^{13}C NMR (DMSO-d_6, 125.8 MHz, trifluoroacetate salt): δ 39.01, 42.12, 45.88 (2×), 52.28 (2×), 109.40, 121.14, 123.52, 124.00, 126.04, 127.28, 127.40, 134.01, 134.54, 146.72, 171.99. IR (FTIR microscope, transmission, trifluoroacetate salt) ν_{max} 3371, 3198, 3032, 2841, 2733, 2621, 2489, 1673, 1624, 1602, 1509, 1458, 1407, 1272, 1235, 1060 cm^{-1}.

3-(1*H*-Indol-3-yl)-4-[3-(4-methylpiperazin-1-yl)naphthalen-1-yl]pyrrole-2,5-dione (7). The monoacetic acid salt of **6** (100 mg, 0.29 mmol) and (1*H*-indol-3-yl)oxoacetic acid methyl ester (89 mg, 0.44 mmol) and 1 cm^3 of dry 3 Å molecular sieves were suspended in THF (2.5 mL). A solution of potassium *tert*-butoxide (1 M in THF, 1.16 mL) was slowly added during 30 min. After an additional 30 min, the reaction mixture was diluted with concentrated aqueous NH_4Cl solution and

extracted with ethyl acetate. The combined organic layers were dried over Na_2SO_4, filtered, and concentrated. Purification by flash chromatography (MeO^tBu/MeOH/aqueous NH_3, 99:1:0.5 to 80:20:0.5, afforded **7** as an orange solid. This material was dissolved in a mixture of MeOH and AcOH. After concentration and azeotropic removal of excess AcOH with MeOH, the monoacetate salt of **7** (95 mg, 66%) was obtained. ES-MS: 437 $[M + H]^+$. HRMS: calcd for $C_{27}H_{25}N_4O_2$ $[M + H]^+$ 437.197 20, found 437.197 30. ^{1}H NMR (DMSO-d_6, 500 MHz, trifluoroacetate salt): δ 2.83 (s, 3H), 2.90−3.10 (m, 4H), 3.45−3.55 (br, 2H), 3.80−3.95 (m, 2H), 6.28 (d, J = 8.3 Hz, 1H), 6.46 (dd, J = 8.3, 7.7 Hz, 1H), 6.92 (dd, J = 8.1, 7.7 Hz, 1H), 7.15 (dd, J = 8.4, 7.7 Hz, 1H), 7.32 (d, J = 8.1 Hz, 1H), 7.34−7.42 (m, 3H), 7.58 (d, J = 8.4 Hz, 1H), 7.80 (d, J = 8.3 Hz, 1H), 7.97 (d, J = 3.0 Hz, 1H), 10.05−10.20 (br s, 1H), 11.16 (s, 1H), 11.90 (s, 1H). ^{13}C NMR (DMSO-d_6, 125.8 MHz, trifluoroacetate salt): δ 42.09, 45.97 (2×), 52.08 (2×), 105.06, 111.61, 112.01, 119.84, 120.64, 121.59, 121.96, 123.91, 124.71, 125.34, 126.46, 126.66, 127.25, 128.31, 130.20, 131.42, 134.26, 135.68, 136.30, 146.56, 172.25, 172.54. IR (FTIR microscope, transmission, trifluoroacetate salt) ν_{max} 3469, 3218, 3054, 2838, 2732, 2631, 2490, 1751, 1707, 1621, 1601, 1510, 1494, 1455, 1432, 1345, 1237, 750 cm^{-1}.

2-(2-Chloroquinolin-4-yl)acetamide (8). Under an atmosphere of argon, (2-oxo-1,2-dihydroquinolin-4-yl)acetic acid methyl ester (9.35 g, 43.0 mmol) was suspended in $POCl_3$ (6.4 mL). The thick suspension was heated to 80 °C for 2 h. After the mixture was cooled to room temperature, the orange suspension was carefully poured onto an ice−water mixture. The mixture was rendered basic by the addition of NaOH (8 M aqueous solution) and extracted with ethyl acetate. The organic layers were washed with H_2O (3×) and brine (2×), dried over Na_2SO_4, filtered, and concentrated to afford crude (2-chloroquinolin-4-yl)acetic acid methyl ester (9.63 g, 95%) pure enough to be used in the next step directly. ES-MS: 236 $[M + H]^+$. ^{1}H NMR ($CDCl_3$, 300 MHz): δ 3.71 (s, 3H), 4.05 (s, 3H), 7.61 (dd, J = 9.2, 8.2 Hz, 1H), 7.75 (dd, J = 9.2, 8.2 Hz, 1H), 7.95 (d, J = 9.2 Hz, 1H), 8.05 (d, J = 9.2 Hz, 1H). (2-Chloroquinolin-4-yl)acetic acid methyl ester (5.45 g, 23.13 mmol) was suspended in aqueous NH_4OH (28%, 110 mL). The mixture was stirred at room temperature for 16 h. After concentration, the solid residue was taken up in hot ethyl acetate. Upon slow cooling to 0 °C, **8** (3.18 g, 62%) separated as a slightly yellow solid. ES-MS: 221 $[M + H]^+$. HRMS: calcd for $C_{11}H_9ClN_2O$ $[M + H]^+$ 221.0482, found 221.0480. ^{1}H NMR (DMSO-d_6, 300 MHz): δ 3.88 (s, 2H), 7.16 (br s, 1H), 7.30 (s, 1H), 7.65 (dd, J = 8.4, 7.5 Hz, 1H), 7.70 (br s, 1H), 7.80 (dd, J = 8.4, 7.5 Hz, 1H), 7.93 (d, J = 8.4 Hz, 1H), 8.12 (d, J = 8.4 Hz, 1H). ^{13}C NMR (DMSO-d_6, 100.7 MHz): δ 38.9, 123.7, 125.0, 126.8, 127.5, 128.8, 131.0, 147.3, 147.7, 149.8, 170.7. IR (KBr) ν_{max} 3305, 3144, 1697, 1401, 1107, 918, 761 cm^{-1}.

2-[2-(4-Methylpiperazin-1-yl)quinolin-4-yl]acetamide (9). **8** (500 mg, 2.27 mmol) was dissolved in 1-methyl-2-pyrrolidinone (3.0 mL). *N*-Methylpiperazine (1.3 mL, 11.33 mmol) was added, and the mixture was stirred at room temperature for 60 h. After dilution with ethyl acetate, the resulting suspension was filtered. The solution was concentrated, and the resulting solid was stirred with hexanes. The remaining solid was combined with the filtered-off solid, and purification by flash chromatography (ethyl acetate/MeOH/aqueous NH_4OH, 80:18:1) afforded **9** (518 mg, 80%) as a slightly tan-colored solid. ES-MS: 285 $[M + H]^+$, HRMS: calcd for $C_{16}H_{20}N_4O$ $[M + H]^+$ 285.1715, found 285.1712. ^{1}H NMR (DMSO-d_6, 400 MHz): δ 2.25 (s, 3H), 2.47 (m, 4H), 3.67 (m, 4H), 3.77 (s, 2H), 7.00 (br s, 1H), 7.16 (s, 1H), 7.22 (dd, J = 8.4, 7.5 Hz, 1H), 7.50 (dd, J = 8.4, 7.5 Hz, 1H), 7.56 (m, 2H), 7.85 (d, J = 8.4 Hz, 1H). IR (KBr) ν_{max} 3337, 1668, 1614, 1403, 1221, 994, 766 cm^{-1}.

3-(1*H*-Indol-3-yl)-4-[2-(4-methylpiperazin-1-yl)quinolin-4-yl]pyrrole-2,5-dione (10). **9** (200 mg, 0.7 mmol) and 3-indoleglyoxylic acid methyl ester (143 mg, 0.7 mmol) were dissolved in *N*,*N*-dimethylformamide (7 mL). Potassium *tert*-butoxide (1.0 M in THF, 3.52 mL, 5 equiv) was added dropwise at 0 °C. The mixture was stirred at 80 °C for 19 h. After dilution with methylene chloride, the organic layer was washed with H_2O (2×) and brine (1×), dried over Na_2SO_4, filtered, and concentrated. The residue was purified by flash chromatography (ethyl acetate/H_2O/AcOH, 50:1:10). The product-containing fractions were concentrated. The residue was dissolved in ethyl acetate, and the solution was washed with aqueous $NaHCO_3$ solution (2×) and brine (2×). After the aqueous layers were back-extracted with ethyl acetate (2×), the combined organic layers were dried over Na_2SO_4, filtered, and concentrated to afford the free base of **10** (190 mg, 62%) as an orange solid. ESI-MS: 438 $[M + H]^+$. HRMS: calcd for $C_{26}H_{23}N_5O_2$ $[M + H]^+$ 438.1930, found 438.1925. ^{1}H NMR (DMSO-d_6, 400 MHz): δ 2.20 (s, 3H), 2.28−2.42 (m, 4H), 3.56−3.72 (m, 4H), 6.56−6.63 (m, 2H), 6.98−7.07 (m, 2H), 7.21 (s, 1H), 7.36 (d, J = 8.0 Hz, 1H), 7.46−7.52 (m, 2H), 7.61 (d, J = 8.3 Hz, 1H), 7.96 (d, J = 2.7 Hz, 1H), 11.23 (s, 1H), 11.90 (s, 1H). ^{13}C NMR (DMSO-d_6, 100.6 MHz): δ 45.0, 46.0, 54.6, 105.2, 112.1, 112.5, 120.4, 121.0, 121.4, 122.5, 122.6, 125.0, 125.7, 126.7, 126.9, 129.9, 132.1, 136.9, 137.7, 139.6, 147.8, 156.8, 172.2, 172.4. IR (KBr) ν_{max} 3330, 1706, 1595, 1432, 1338, 1234, 1000, 751 cm^{-1}.

2-(3-Chloroisoquinolin-1-yl)acetamide (11). Sodium hydride (60% in mineral oil, 2.0 g, 50 mmol) was suspended in xylene (100 mL). A solution of malonic acid diethyl ester (8.65 g, 54.0 mmol) in xylene (20 mL) was added dropwise at room temperature. The mixture was heated to 80 °C for 30 min. 1,3-Dichloroisoquinoline (3.6 g, 18.2 mmol) dissolved in xylene (50 mL) was added dropwise at 80 °C. The solution was heated to 140 °C for 3 h. After the mixture was cooled to room temperature, the solvent was removed and the residue was taken up in ethyl acetate. After the mixture was washed with aqueous $NaHCO_3$ solution, the organic layer was dried over Na_2SO_4, filtered, and concentrated. Purification by flash chromatography (toluene/ethyl acetate, 95:5) afforded (3-chloroisoquinolin-1-yl)acetic acid ethyl ester (2.81 g, 62%) as a viscous oil. ES-MS: 250 $[M + H]^+$. HRMS: calcd for $C_{13}H_{13}NO_2Cl$ $[M + H]^+$ 250.062 93, found 250.063 03. ^{1}H NMR (DMSO-d_6, 600 MHz): δ 1.18 (t, J = 7.3 Hz, 3H), 4.12 (q, J = 7.3 Hz, 2H), 4.39 (s, 2H), 7.70−7.73 (m, 1H), 7.82−7.85 (m, 1H), 7.97−8.00 (m, 2H), 8.21 (d, J = 8.8 Hz, 1H). ^{13}C NMR (DMSO-d_6, 150.9 MHz): δ 14.0, 40.7, 60.6, 119.2, 125.8, 125.9, 126.6, 128.0, 131.4, 138.0, 143.0, 156.3, 169.7. IR (FTIR) ν_{max} 3068, 2981, 2936, 1726, 1579, 1557, 1367, 1335, 1214, 1196, 1021, 754 cm^{-1}. A solution of (3-chloroisoquinolin-1-yl)acetic acid ethyl ester (1.0 g, 4.1 mmol) in NH_3 (approximately 4 M in MeOH, 50 mL) was heated to 130 °C in a stainless steel pressure reactor for 16 h. After the mixture was cooled and carefully concentrated, the residue was crystallized from EtOH to afford **11** (684 mg, 76%). ES-MS: 221 $[M + H]^+$. HRMS: calcd for $C_{11}H_{10}NO_2Cl$ $[M + H]^+$ 221.047 62, found 221.047 60. ^{1}H NMR (DMSO-d_6, 600 MHz): δ 4.14 (s, 2H), 7.13 (br s, 1H), 7.68−7.71 (m, 2H), 7.79−7.82 (m, 2H), 7.93 (s, 1H), 7.96 (d, J = 8.0 Hz, 1H), 8.25 (d, J = 8.4 Hz, 1H). ^{13}C NMR (DMSO-d_6, 150.9 MHz): δ 42.1, 118.7, 126.3 (2×), 126.5, 127.7, 131.2, 137.9, 143.1, 158.2, 170.5. IR (FTIR) ν_{max} 3353, 3175, 2942, 1675, 1620, 1583, 1557, 916, 749, 665 cm^{-1}.

3-(3-Chloroisoquinolin-1-yl)-4-(1*H*-indol-3-yl)pyrrole-2,5-dione (12). **11** (440 mg, 2.0 mmol) and (1*H*-indol-3-yl)oxoacetic acid methyl ester (1.0 g, 4.9 mmol) were dissolved in THF (15 mL). After the mixture was heated to 80 °C, potassium *tert*-butoxide (1 M in THF, 10 mL) was added dropwise, and heating to reflux was continued for 1 h. The reaction mixture was concentrated, taken up in ethyl acetate, and washed with aqueous $NaHCO_3$ solution. The organic layer was dried over Na_2SO_4, filtered, and concentrated. **12** (400 mg, 54%) was obtained as a red solid by crystallization from diethyl ether. ES-MS: 374 $[M + H]^+$. HRMS: calcd for $C_{21}H_{13}ClN_3O_2$ $[M + H]^+$ 374.069 08, found 374.069 15. ^{1}H NMR (DMSO-d_6, 600 MHz): δ 5.98 (d, J = 8.1 Hz, 1H), 6.50 (dd, J = 8.1, 6.6 Hz, 1H), 6.95 (dd, J = 8.1, 6.6 Hz, 1H), 7.35 (d, J = 8.1 Hz, 1H), 7.49−7.52 (m, 1H), 7.73−7.76 (m, 1H), 7.97−8.00 (m, 2H), 8.15 (br s, 2H), 11.32 (s, 1H), 12.04 (s, 1H). ^{13}C NMR (DMSO-d_6, 150.9 MHz): δ 104.9, 112.5, 119.5, 120.4, 122.4,

124.7, 126.5, 126.7, 126.8, 128.3, 131.9, 132.6, 136.5, 137.5, 138.0, 143.7, 153.1, 171.8, 171.9. IR (FTIR, transmission) ν_{max} 3170, 3061, 2934, 1764, 1710, 1623, 1578, 1551, 1513, 1340, 1330, 749 cm^{-1}.

3-(1*H*-Indol-3-yl)-4-[3-(4-methylpiperazin-1-yl)isoquinolin-1-yl]pyrrole-2,5-dione (13). 12 (90 mg, 0.24 mmol) was dissolved in *N*-methylpiperazine (1.5 mL). The solution was heated to 130 °C for 18 h. After concentration, the residue was dissolved in ethyl acetate and washed with aqueous $NaHCO_3$ and then extracted into aqueous HCl (0.2 M). The aqueous phase was carefully rendered basic by the addition of solid $NaHCO_3$ and then extracted with methylene chloride. The combined organic layers were dried over Na_2SO_4, filtered, and concentrated. Purification by flash chromatography (CH_2Cl_2/MeOH/aqueous NH_3, 91:1:1 to 82:2:2) afforded the free base of **13** (30 mg, 29%) as a dark red solid. ES-MS: 438 $[M + H]^+$. HRMS: calcd for $C_{26}H_{24}N_5O_2$ $[M + H]^+$ 438.192 45, found 438.192 43. ^{1}H NMR (DMSO-d_6, 600 MHz): δ 2.75 (s, 3H), 2.90−3.15 (br, 4H), 3.35−3.50 (br, 2H), 4.25−4.35 (br, 2H), 6.03 (d, J = 8.1 Hz, 1H), 6.51 (dd, J = 8.1, 6.9 Hz, 1H), 6.96 (dd, J = 8.0, 6.9 Hz, 1H), 7.17−7.19 (m, 1H), 7.29 (s, 1H), 7.35 (d, J = 8.0 Hz, 1H), 7.52−7.55 (m, 1H), 7.74−7.76 (m, 2H), 8.10 (d, J = 2.9 Hz, 1H), 10.10−10.20 (br, 1H), 11.22 (s, 1H), 12.04 (s, 1H). ^{13}C NMR (DMSO-d_6, 150.9 MHz): δ 42.2, 42.9, 51.8, 100.9, 105.1, 112.3, 120.0, 120.2, 122.2, 122.9, 124.2, 124.9, 125.9, 126.6, 130.7, 132.2, 136.5, 136.8, 138.9, 150.8, 153.9, 172.1, 172.3. IR (FTIR, transmission) ν_{max} 2854, 2733, 2491, 1758, 1712, 1625, 1583, 1447, 1343, 750 cm^{-1}.

3-(1*H*-Indol-3-yl)-4-[5-methyl-2-(4-methylpiperazin-1-yl)-quinazolin-4-yl]pyrrole-2,5-dione (14). 14 was synthesized as described for **1** but starting from commercially available 5-methyl-1*H*-quinazoline-2,4-dione. ES-MS: 453 $[M + H]^+$. ^{1}H NMR (DMSO-d_6, 400 MHz): δ 2.13 (s, 3H), 2.18−2.26 (m, 4H), 2.49 (s, 3H), 3.59−3.78 (m, 4H), 6.66−6.73 (m, 2H), 7.04−7.09 (m, 2H), 7.41−7.47 (m, 2H), 7.58−7.62 (m, 1H), 8.05 (s, 1H), 11.25−11.50 (br, 1H), 11.90−12.10 (br, 1H).

3-[6-Fluoro-2-(4-methylpiperazin-1-yl)quinazolin-4-yl]-4-(1*H*-indol-3-yl)pyrrole-2,5-dione (15). 15 was synthesized as described for **1** but starting from commercially available 6-fluoro-1*H*-quinazoline-2,4-dione. EI-MS: 456 $[M + H]^+$. HRMS: calcd for $C_{25}H_{21}FN_6O_2$ $[M + H]^+$ 457.1788, found 457.1785. ^{1}H NMR (DMSO-d_6, 400 MHz): δ 2.11−2.20 (br, 4H), 2.14 (s, 3H), 3.62−3.71 (br, 4H), 6.29 (d, J = 8.0 Hz, 1H), 6.66 (dd, J = 8.0, 7.0 Hz, 1H), 7.04 (dd, J = 8.0, 7.0 Hz, 1H), 7.40 (d, J = 8.0 Hz, 1H), 7.54−7.61 (m, 3H), 8.16 (s, 1H), 11.26 (br s, 1H), 12.05 (br s, 1H). ^{13}C NMR (DMSO-d_6, 100.6 MHz): δ 44.0, 46.1, 54.5, 105.3, 110.8 (d, J = 22.8 Hz), 112.8, 118.4 (d, J = 9.3 Hz), 120.3, 120.8, 122.8, 124.2, 124.8, 125.0, 128.5 (d, J = 8.3 Hz), 133.2, 136.9, 138.6, 150.1, 155.8, 158.3 (d, J = 10.5 Hz), 162.1 (d, J = 4.9 Hz), 171.7, 172.1. IR (KBr) ν_{max} 3350, 1710, 1549, 1338, 1002, 745 cm^{-1}.

3-[6-Chloro-2-(4-methylpiperazin-1-yl)quinazolin-4-yl]-4-(1*H*-indol-3-yl)pyrrole-2,5-dione (16). 16 was synthesized as described for **1** but starting from commercially available 6-chloro-1*H*-quinazoline-2,4-dione. ES-MS: 471 $[M - H]^-$. HRMS: calcd for $C_{25}H_{21}ClN_6O_2$ $[M + H]^+$ 473.1493, found 473.1489. ^{1}H NMR (DMSO-d_6, 400 MHz): δ 2.04−2.22 (br s, 7H), 3.56−3.72 (br, 4H), 6.27 (d, J = 8.0 Hz, 1H), 6.67 (dd, J = 8.0, 7.1 Hz, 1H), 7.05 (dd, J = 8.0, 7.1 Hz, 1H), 7.41 (d, J = 8.0 Hz, 1H), 7.54 (d, J = 9.2 Hz, 1H), 7.66 (d, J = 9.2, 2.1 Hz, 1H), 7.85 (d, J = 2.1 Hz, 1H), 8.17 (s, 1H), 11.2−11.3 (br, 1H), 12.0−12.1 (br, 1H). ^{13}C NMR (DMSO-d_6, 100.7 MHz): δ 43.9, 46.0, 54.4, 105.4, 112.9, 119.1, 120.4, 120.8, 122.8, 123.9, 125.0, 126.3, 126.4, 128.0, 133.4, 135.3, 137.0, 138.9, 151.5, 158.4, 161.9, 171.8, 172.0. IR (KBr) ν_{max} 3350, 1709, 1545, 1339, 1001, 746 cm^{-1}.

3-(1*H*-Indol-3-yl)-4-[6-methyl-2-(4-methylpiperazin-1-yl)quinazolin-4-yl]pyrrole-2,5-dione (17). 17 was synthesized as described for **1** but starting from commercially available 6-methyl-1*H*-quinazoline-2,4-dione. ES-MS: 451 $[M - H]^-$. HRMS: calcd for $C_{26}H_{24}N_6O_2$ $[M + H]^+$ 453.2039, found 453.2042. ^{1}H NMR (DMSO-d_6, 400 MHz): δ 2.12−2.22 (br, 4H), 2.13 (s, 3H), 2.28 (s, 3H), 3.62−3.72 (br, 4H), 6.38 (d, J = 8.2 Hz, 1H), 6.65 (dd, J = 8.2, 7.1 Hz, 1H), 7.04 (dd, J = 8.2, 7.1 Hz, 1H), 7.40 (d, J = 8.2 Hz, 1H), 7.47 (d, J = 8.4 Hz, 1H), 7.52 (d, J = 1.8 Hz, 1H), 7.53 (dd, J = 8.4, 1.8 Hz, 1H), 8.13 (s, 1H), 11.26 (br s, 1H), 12.01 (br s, 1H). ^{13}C NMR (DMSO-d_6, 100.6 MHz): δ 21.6, 44.5, 46.6, 55.0, 105.9, 113.3, 119.3, 121.0, 121.3, 123.3, 125.6, 125.7, 126.3, 126.4, 132.6, 133.5, 137.4, 137.5, 138.7, 151.8, 158.7, 162.3, 172.4, 172.8. IR (KBr) ν_{max} 2919, 2850, 1708, 1548, 1442, 1338, 1002, 744 cm^{-1}.

3-(1*H*-Indol-3-yl)-4-[6-isopropyl-2-(4-methylpiperazin-1-yl)quinazolin-4-yl]pyrrole-2,5-dione (18). 18 was synthesized as described for **1**. The starting 6-isopropyl-1*H*-quinazoline-2,4-dione was prepared from commercially available 2-amino-5-isopropylbenzoic acid as described.[25] ES-MS: 479 $[M - H]^-$. HRMS: calcd for $C_{28}H_{28}N_6O_2$ $[M + H]^+$ 481.2352, found 481.2357. ^{1}H NMR (DMSO-d_6, 400 MHz): δ 0.97 (d, J = 6.9 Hz, 6H), 2.17 (s, 3H), 2.18−2.28 (br, 4H), 2.74 (hept, J = 6.9 Hz, 1H), 3.67−3.77 (br, 4H), 6.29 (d, J = 8.2 Hz, 1H), 6.61 (dd, J = 8.2, 7.1 Hz, 1H), 7.00 (dd, J = 8.2, 7.1 Hz, 1H), 7.36 (d, J = 8.2 Hz, 1H), 7.38 (d, J = 2.0 Hz, 1H), 7.45 (d, J = 8.8 Hz, 1H), 7.53 (dd, J = 8.8, 2.0 Hz, 1H), 8.10 (s, 1H), 11.26 (br s, 1H), 12.00 (br s, 1H). ^{13}C NMR (DMSO-d_6, 100.6 MHz): δ 23.7, 33.1, 44.0, 46.2, 54.6, 105.5, 112.6, 118.3, 120.3, 120.6, 122.7, 123.0, 124.8, 125.1, 125.9, 132.7, 134.4, 136.9, 138.3, 142.5, 151.5, 158.2, 161.5, 171.7, 172.2. IR (KBr) ν_{max} 3331, 2957, 1711, 1549, 1446, 1340, 1237, 1139, 1003, 744 cm^{-1}.

3-[6-*tert*-Butyl-2-(4-methylpiperazin-1-yl)quinazolin-4-yl]-4-(1*H*-indol-3-yl)pyrrole-2,5-dione (19). 19 was synthesized as described for **1**. The starting 6-*tert*-butyl-1*H*-quinazoline-2,4-dione was prepared from commercially available 2-amino-5-*tert*-butylbenzoic acid using known procedures.[25] ES-MS: 493 $[M - H]^-$. HRMS: calcd for $C_{29}H_{30}N_6O_2$ $[M + H]^+$ 495.2508, found 495.2510. ^{1}H NMR (DMSO-d_6, 400 MHz): δ 1.02 (s, 9H), 2.19 (s, 3H), 2.22−2.35 (br, 1H), 3.70−3.80 (br, 1H), 6.21 (d, J = 8.0 Hz, 1H), 6.21 (d, J = 8.0 Hz, 1H), 6.60 (dd, J = 8.0, 7.0 Hz, 1H), 6.98 (dd, J = 8.1, 7.0 Hz, 1H), 7.36 (d, J = 8.1 Hz, 1H), 7.37 (s, 1H), 7.44 (d, J = 9.0 Hz, 1H), 7.67 (dd, J = 9.0, 1.6 Hz, 1H), 8.12 (s, 1H), 11.2−11.4 (br, 1H), 11.9−12.2 (br, 1H). ^{13}C NMR (DMSO-d_6, 100.7 MHz): δ 30.8, 34.4, 44.0, 46.2, 54.6, 105.6, 112.5, 117.9, 120.2, 120.6, 121.7, 122.7, 124.5, 125.1, 125.7, 132.8, 133.2, 136.8, 138.2, 144.6, 151.1, 158.3, 161.5, 171.6, 172.1. IR (KBr) ν_{max} 3328, 2953, 1711, 1548, 1445, 1341, 1247, 1142, 1003, 744 cm^{-1}.

3-[7-Fluoro-2-(4-methylpiperazin-1-yl)quinazolin-4-yl]-4-(1*H*-indol-3-yl)pyrrole-2,5-dione (20). 20 was synthesized as described for **1** but starting from commercially available 7-fluoro-1*H*-quinazoline-2,4-dione. ES-MS: 457 $[M + H]^+$. HRMS: calcd for $C_{25}H_{21}FN_6O_2$ $[M + H]^+$ 457.1788, found 457.1786. ^{1}H NMR (DMSO-d_6, 400 MHz): δ 2.06−2.20 (br, 4H), 2.13 (s, 3H), 3.60−3.76 (br, 4H), 6.32 (d, J = 8.0 Hz, 1H), 6.67 (dd, J = 8.0, 7.0 Hz, 1H), 6.95−7.01 (m, 1H), 7.05 (dd, J = 8.0, 7.0 Hz, 1H), 7.23−7.26 (dd, J = 10.8, 2.3 Hz, 1H), 7.41 (d, J = 8.0 Hz, 1H), 7.81−7.85 (m, 1H), 8.16 (s, 1H), 11.28 (br s, 1H), 12.05 (br s, 1H). ^{13}C NMR (DMSO-d_6, 100.6 MHz): δ 44.8, 47.0, 55.4, 106.2, 110.3 (J = 20.6 Hz), 113.5 (J = 25.1 Hz), 117.0, 121.3, 121.8, 123.8, 125.1, 126.0, 131.7 (J = 11.5 Hz), 134.2, 137.9, 139.5, 155.6 (J = 14.7 Hz), 159.6, 163.2, 167.1 (J = 252.3 Hz), 172.6, 173.0. IR (KBr) ν_{max} 2940, 1710, 1626, 1555, 1491, 1332, 1004, 745 cm^{-1}.

3-[7-Chloro-2-(4-methylpiperazin-1-yl)quinazolin-4-yl]-4-(1*H*-indol-3-yl)pyrrole-2,5-dione (21). 21 was synthesized as described for **1** but starting from commercially available 7-chloro-1*H*-quinazoline-2,4-dione. ES-MS: 471 $[M - H]^-$. HRMS: calcd for $C_{25}H_{21}ClN_6O_2$ $[M + H]^+$ 473.1493, found 473.1491. ^{1}H NMR (DMSO-d_6, 400 MHz): δ 2.08−2.22 (br, 4H), 2.13 (s, 3H), 3.61−3.78 (br, 4H), 6.29 (d, J = 8.0 Hz, 1H), 6.69 (dd, J = 8.0, 7.0 Hz, 1H), 7.06 (dd, J = 8.2, 7.0 Hz, 1H), 7.11 (dd, J = 8.8, 1.6 Hz, 1H), 7.42 (d, J = 8.2 Hz, 1H), 7.58 (d, J = 1.6 Hz, 1H), 7.77 (d, J = 8.8 Hz, 1H), 8.18 (s, 1H), 11.31 (br s, 1H), 12.08 (br s, 1H). ^{13}C NMR (DMSO-d_6, 100.6 MHz): δ 43.9, 46.0, 54.5,

105.9, 112.9, 117.2, 120.3, 120.9, 122.9, 123.1, 123.9, 124.5, 125.0, 129.6, 133.4, 137.0, 138.7, 139.6, 153.6, 158.7, 162.6, 171.7, 172.0. IR (KBr) ν_{max} 3200, 1761, 1692, 1606, 1544, 752 cm^{-1}.

3-(1*H*-Indol-3-yl)-4-[8-methyl-2-(4-methylpiperazin-1-yl)quinazolin-4-yl]pyrrole-2,5-dione (22). **22** was synthesized as described for **1** but starting from commercially available 8-methyl-1*H*-quinazoline-2,4-dione. ES-MS: 451 $[M - H]^-$. HRMS: calcd for $C_{26}H_{24}N_6O_2$ $[M + H]^+$ 453.2039, found 453.2041. ^{1}H NMR (DMSO-d_6, 400 MHz): δ 2.15 (s, 3H), 2.16−2.26 (br, 4H), 2.53 (s, 3H), 3.67−3.78 (br, 4H), 6.47 (d, J = 8.2 Hz, 1H), 6.66 (dd, J = 8.2, 6.9 Hz, 1H), 6.97−7.05 (m, 2H), 7.38 (d, J = 8.0 Hz, 1H), 7.52−7.54 (m, 2H), 8.08 (s, 1H), 11.25 (br s, 1H), 11.99 (br s, 1H). ^{13}C NMR (DMSO-d_6, 100.6 MHz): δ 17.2, 44.0, 46.1, 54.5, 105.3, 112.7, 118.3, 120.5, 120.8, 122.3, 122.8, 124.9, 125.2, 125.3, 132.8, 133.5, 134.3, 136.9, 138.1, 151.6, 157.9, 162.8, 171.8, 172.1. IR (KBr) ν_{max} 3142, 1688, 1617, 1553, 1428, 760 cm^{-1}.

3-(4-Chloro-1*H*-indol-3-yl)-4-[2-(4-methylpiperazin-1-yl)-quinazolin-4-yl]pyrrole-2,5-dione (23). **23** was synthesized as described for **1**, but the final cyclocondensation was conducted with commercially available (4-chloro-1*H*-indol-3-yl)oxoacetic acid methyl ester. ES-MS: 473 $[M + H]^+$. HRMS: calcd for $C_{25}H_{22}ClN_6O_2$ $[M + H]^+$ 473.148 73, found 473.148 99. ^{1}H NMR (DMSO-d_6, 600 MHz): δ 2.82 (s, 3H), 2.90−3.10 (br, 2H), 3.25−3.35 (br, 2H), 3.45−3.55 (br, 2H), 4.70−4.85 (br, 2H), 7.06 (d, J = 7.7 Hz, 1H), 7.12 (dd, J = 8.1, 7.7 Hz, 1H), 7.19−7.22 (m, 1H), 7.39 (d, J = 8.1 Hz, 1H), 7.52 (br s, 1H), 7.56 (d, J = 8.4 Hz, 1H), 7.70−7.73 (m, 2H), 10.30−10.45 (br, 1H), 11.53 (s, 1H), 12.03 (s, 1H). ^{13}C NMR (DMSO-d_6, 150.9 MHz): δ 40.9, 42.3, 52.0, 102.4, 111.4, 118.1, 120.8, 123.2, 123.5, 123.7, 124.7, 125.8, 126.6, 129.9, 133.3, 135.0, 137.7, 141.0, 151.9, 157.2, 160.9, 170.7, 171.6. IR (FTIR, transmission) ν_{max} 3202, 3041, 2730, 2486, 1766, 1720, 1618, 1571, 1553, 1485, 1455, 756 cm^{-1}.

3-(5-Chloro-1*H*-indol-3-yl)-4-[2-(4-methylpiperazin-1-yl)-quinazolin-4-yl]pyrrole-2,5-dione (24). **24** was synthesized as described for **1**, but the final cyclocondensation was conducted with commercially available (5-chloro-1*H*-indol-3-yl)oxoacetic acid methyl ester. ES-MS: 473 $[M + H]^+$. HRMS: calcd for $C_{25}H_{22}ClN_6O_2$ $[M + H]^+$ 473.148 73, found 473.148 92. ^{1}H NMR (DMSO-d_6, 600 MHz): δ 2.70−3.00 (br, 2H), 2.79 (s, 3H), 3.15−3.35 (br, 2H), 3.40−3.55 (br, 2H), 4.70−4.80 (br, 2H), 6.31 (br s, 1H), 7.06 (dd, J = 8.4, 1.8 Hz, 1H), 7.19 (dd, J = 8.1, 7.0 Hz, 1H), 7.41 (d, J = 8.4 Hz, 1H), 7.64 (d, J = 8.4 Hz, 1H), 7.74 (dd, J = 8.4, 7.0 Hz, 1H), 7.78 (d, J = 8.1 Hz, 1H), 8.16 (d, J = 2.9 Hz, 1H), 10.30−10.45 (br, 1H), 11.41 (s, 1H), 12.34 (s, 1H). ^{13}C NMR (DMSO-d_6, 150.9 MHz): δ 41.0, 42.4, 52.2, 104.4, 114.1, 118.9, 119.7, 122.4, 123.7, 124.8, 125.0, 125.9, 127.0, 134.1, 135.0, 135.2, 137.7, 152.1, 157.5, 162.7, 171.3, 171.6. IR (FTIR, transmission) ν_{max} 3166, 3037, 2730, 1760, 1716, 1620, 1570, 1551, 1484, 1456, 1429, 757 cm^{-1}.

3-(6-Chloro-1*H*-indol-3-yl)-4-[2-(4-methylpiperazin-1-yl)-quinazolin-4-yl]pyrrole-2,5-dione (25). **25** was synthesized as described for **1**, but the final cyclocondensation was conducted with commercially available (6-chloro-1*H*-indol-3-yl)oxoacetic acid methyl ester. ES-MS: 473 $[M + H]^+$. HRMS: calcd for $C_{25}H_{22}ClN_6O_2$ $[M + H]^+$ 473.148 73, found 473.148 83. ^{1}H NMR (DMSO-d_6, 600 MHz): δ 2.05−2.25 (br, 4H), 2.12 (s, 3H), 3.60−3.80 (br, 4H), 6.35 (d, J = 8.1 Hz, 1H), 6.68 (d, J = 8.1 Hz, 1H), 7.10 (dd, J = 8.1, 6.9 Hz, 1H), 7.45 (s, 1H), 7.54 (d, J = 8.5 Hz, 1H), 7.67 (dd, J = 8.5, 6.9 Hz, 1H), 7.72 (d, J = 8.1 Hz, 1H), 8.11 (s, 1H), 11.25−11.50 (br, 1H), 11.95−12.20 (br, 1H). ^{13}C NMR (DMSO-d_6, 150.9 MHz): δ 43.6, 45.8, 54.2, 105.0, 112.2, 118.1, 120.6, 121.4, 122.5, 123.5, 125.5, 125.7, 127.1, 133.5, 134.7, 137.1, 137.7, 152.5, 157.9, 161.8, 171.4, 171.6. IR (FTIR, transmission) ν_{max} 3190, 2946, 2805, 1769, 1757, 1696, 1619, 1568, 1550, 1505, 1485, 1342, 759 cm^{-1}.

3-(7-Chloro-1*H*-indol-3-yl)-4-[2-(4-methylpiperazin-1-yl)-quinazolin-4-yl]pyrrole-2,5-dione (26). **26** was synthesized as described for **1**, but the final cyclocondensation was conducted with commercially available (7-chloro-1*H*-indol-3-yl)oxoacetic acid methyl ester. ES-MS: 473 $[M + H]^+$. HRMS: calcd for $C_{25}H_{22}ClN_6O_2$ $[M + H]^+$ 473.148 73, found 473.148 95. ^{1}H NMR (DMSO-d_6, 600 MHz): δ 2.79 (s, 3H), 3.10−3.35 (br, 2H), 3.35−3.65 (br, 4H), 4.65−4.80 (br, 2H), 6.36 (d, J = 8.4 Hz, 1H), 6.70 (dd, J = 8.4, 7.8 Hz, 1H), 7.13 (d, J = 7.8 Hz, 1H), 7.17 (dd, J = 8.4, 6.6 Hz, 1H), 7.61 (d, J = 8.4 Hz, 1H), 7.72−7.74 (m, 1H), 7.79 (d, J = 8.4 Hz, 1H), 8.08 (d, J = 3.3 Hz, 1H), 10.30−10.45 (br, 1H), 11.46 (s, 1H), 12.51 (s, 1H). ^{13}C NMR (DMSO-d_6, 150.9 MHz): δ 41.0, 42.4, 52.2, 105.9, 116.9, 118.8, 119.1, 121.6, 122.2, 123.7, 125.9, 126.0, 126.8, 127.2, 133.3, 133.5, 135.3, 137.8, 152.2, 157.6, 162.4, 171.3, 171.6. IR (FTIR, transmission) ν_{max} 3062, 2871, 2730, 2489, 1761, 1716, 1621, 1551, 1485, 1433, 1343, 784 cm^{-1}.

3-(7-Methyl-1*H*-indol-3-yl)-4-[2-(4-methylpiperazin-1-yl)-quinazolin-4-yl]pyrrole-2,5-dione (27). **27** was synthesized as described for **1**, but the final cyclocondensation was conducted with commercially available (7-methyl-1*H*-indol-3-yl)oxoacetic acid methyl ester. ES-MS: 453 $[M + H]^+$. HRMS: calcd for $C_{26}H_{25}N_6O_2$ $[M + H]^+$ 453.203 35, found 453.203 43. ^{1}H NMR (DMSO-d_6, 600 MHz): δ 2.42 (s, 3H), 2.60−2.90 (br, 2H), 2.75 (s, 3H), 3.10−3.25 (br, 2H), 3.25−3.50 (br, 2H), 4.60−4.80 (br, 2H), 6.04 (d, J = 8.1 Hz, 1H), 6.54 (dd, J = 8.1, 7.0 Hz, 1H), 6.83 (d, J = 7.0 Hz, 1H), 7.20 (dd, J = 8.0, 7.4 Hz, 1H), 7.62 (d, J = 8.4 Hz, 1H), 7.74 (dd, J = 7.4 Hz, 1H), 7.81 (d, J = 8.0 Hz, 1H), 8.14 (d, J = 3.0 Hz, 1H), 10.18−10.28 (br, 1H), 11.36 (br s, 1H), 12.21 (br s, 1H). ^{13}C NMR (DMSO-d_6, 150.9 MHz): δ 16.6, 40.9, 42.3, 52.0, 105.4, 117.5, 118.9, 120.7, 122.0, 123.2, 123.5, 123.8, 124.5, 125.8, 127.3, 132.8, 135.0, 136.1, 138.2, 152.1, 157.4, 162.7, 171.4, 171.8. IR (FTIR, transmission) ν_{max} 2956, 2730, 2485, 1760, 1714, 1619, 1551, 1485, 1345, 784, 757 cm^{-1}.

3-(1-Methyl-1*H*-indol-3-yl)-4-[2-(4-methylpiperazin-1-yl)-quinazolin-4-yl]pyrrole-2,5-dione (28). **28** was synthesized as described for **1**, but the final cyclocondensation was conducted with commercially available (1-methyl-1*H*-indol-3-yl)oxoacetic acid methyl ester. ESI-MS: 453 $[M + H]^+$. HRMS: calcd for $C_{26}H_{24}N_6O_2$ $[M + H]^+$ 453.2039, found 453.2045. ^{1}H NMR (DMSO-d_6, 400 MHz): δ 2.14 (s, 3H), 2.14−2.22 (br, 4H), 3.64−3.76 (br, 4H), 3.88 (s, 3H), 6.28 (d, J = 8.0 Hz, 1H), 6.68 (dd, J = 8.0, 7.0 Hz, 1H), 7.08−7.12 (m, 2H), 7.45 (d, J = 8.4 Hz, 1H), 7.53 (d, J = 8.4 Hz, 1H), 7.65−7.71 (m, 2H), 8.24 (s, 1H), 11.29 (br, 1H). ^{13}C NMR (DMSO-d_6, 125.8 MHz): δ 33.2, 43.6, 45.8, 54.2, 104.0, 110.9, 118.4, 120.1, 120.8, 122.5, 122.6, 123.9, 125.2, 125.6, 127.0, 134.8, 136.4, 137.2, 137.4, 152.4, 158.0, 162.2, 171.5, 171.8. IR (KBr) ν_{max} 2960, 1707, 1548, 1333, 1005, 749 cm^{-1}.

3-(1-Isopropyl-1*H*-indol-3-yl)-4-[2-(4-methylpiperazin-1-yl)-quinazolin-4-yl]pyrrole-2,5-dione (29). **29** was synthesized as described for **1**, but the final cyclocondensation was conducted with (1-isopropyl-1*H*-indol-3-yl)oxoacetic acid methyl ester, which was synthesized from 1-isopropyl-1*H*-indole[26] as described.[27] ES-MS: 481 $[M + H]^+$. HRMS: calcd for $C_{28}H_{28}N_6O_2$ $[M + H]^+$ 481.2352, found 481.2358. ^{1}H NMR (DMSO-d_6, 400 MHz): δ 1.48 (d, J = 6.6 Hz, 6H), 2.05−2.15 (br, 4H), 2.13 (s, 3H), 3.60−3.70 (br, 4H), 4.83 (h, J = 6.6 Hz, 1H), 6.40 (d, J = 8.2 Hz, 1H), 6.68−6.72 (m, 1H), 7.08−7.16 (m, 2H), 7.54−7.58 (m, 2H), 7.68−7.72 (m, 1H), 7.74 (d, J = 8.3, 1H), 8.20 (s, 1H), 11.28−11.34 (br s, 1H). ^{13}C NMR (DMSO-d_6, 100.7 MHz): δ 22.4, 43.9, 46.1, 47.8, 54.5, 105.0, 111.4, 118.6, 120.7, 121.1, 122.7, 122.8, 124.9, 125.7, 125.9, 127.4, 131.7, 134.9, 136.3, 138.2, 152.9, 158.3, 162.3, 171.7, 172.1. IR (KBr) ν_{max} 1717, 1547, 1300, 1234, 1214, 1002, 738 cm^{-1}.

3-(2-Methyl-1*H*-indol-3-yl)-4-[2-(4-methylpiperazin-1-yl)-quinazolin-4-yl]pyrrole-2,5-dione (30). **30** was synthesized as described for **1**, but the final cyclocondensation was conducted with commercially available (2-methyl-1*H*-indol-3-yl)oxoacetic acid methyl ester. ES-MS: 453 $[M + H]^+$. HRMS: calcd for $C_{26}H_{24}N_6O_2$ $[M + H]^+$ 453.2039, found 453.2044. ^{1}H NMR (DMSO-d_6, 400 MHz): δ 2.20 (s, 3H), 2.21 (s, 3H), 2.27−2.33 (br, 4H), 3.75−3.82 (br, 4H), 6.76−6.80 (m, 1H), 6.95−6.99 (m, 1H), 7.00−7.03 (m, 1H), 7.11 (d, J = 7.9 Hz,

1H), 7.20 (d, J = 8.1 Hz, 1H), 7.45 (d, J = 8.5 Hz, 1H), 7.56−7.64 (m, 2H), 11.33 (br, 1H), 11.56 (br s, 1H). ^{13}C NMR (DMSO-d_6, 100.6 MHz): δ 14.2, 44.6, 46.7, 55.3, 102.7, 111.8, 118.2, 120.0, 120.6, 122.2, 123.3, 126.5, 127.3, 127.7, 131.3, 135.3 (2x), 136.5, 140.0, 141.2, 159.0, 162.6, 171.8, 172.1. IR (KBr) ν_{max} 2938, 1715, 1549, 1339, 1003, 754 cm^{-1}.

3-(1*H*-Indol-3-yl)-4-(2-piperazin-1-yl-quinazolin-4-yl)pyrrole-2,5-dione (31). **31** was synthesized as described for **1** but using piperazine instead of *N*-methylpiperazine in the reaction with 2-(2-chloroquinazolin-4-yl)acetamide. ES-MS: 423 $[M - H]^-$. HRMS: calcd for $C_{24}H_{20}N_6O_2$ $[M + H]^+$ 425.1726, found 425.1720. ^{1}H NMR (DMSO-d_6, 400 MHz): δ 2.56−2.66 (br, 4H), 3.55−3.75 (br, 4H), 6.41 (d, J = 8.0 Hz, 1H), 6.66 (dd, J = 8.0, 7.2 Hz, 1H), 7.01−7.05 (m, 1H), 7.07 (dd, J = 8.0, 7.2 Hz, 1H), 7.39 (d, J = 8.0 Hz, 1H), 7.52 (d, J = 8.6 Hz, 1H), 7.63−7.69 (m, 2H), 8.13 (br s, 1H), 11.8−12.2 (br, 1H). ^{13}C NMR (DMSO-d_6, 100.7 MHz): δ 45.2, 45.7, 105.3, 112.8, 118.6, 120.5, 120.7, 122.6, 122.7, 124.8, 125.1, 125.9, 127.3, 133.0, 134.8, 136.9, 138.2, 152.7, 158.4, 162.5, 171.8, 172.2. IR (KBr) ν_{max} 3310, 1709, 1548, 1337, 750 cm^{-1}.

3-(1-Methyl-1*H*-indol-3-yl)-4-(2-piperazin-1-yl-quinazolin-4-yl)pyrrole-2,5-dione (32). **32** was synthesized as described for **1** but using 2-(2-piperazin-1-yl-quinazolin-4-yl)acetamide and (1-methyl-1*H*-indol-3-yl)oxoacetic acid methyl ester in the final cyclocondensation. ES-MS: 439 $[M + H]^+$. HRMS: calcd for $C_{25}H_{22}N_6O_2$ $[M + H]^+$ 439.1882, found 439.1879. ^{1}H NMR (DMSO-d_6, 400 MHz): δ 2.58−2.66 (br, 4H), 3.62−3.70 (br, 4H), 3.89 (s, 3H), 6.34 (d, J = 8.2 Hz, 1H), 6.69 (dd, J = 8.2, 7.1 Hz, 1H), 7.06−7.12 (m, 2H), 7.46 (d, J = 8.2 Hz, 1H), 7.52 (d, J = 8.4 Hz, 1H), 7.63−7.69 (m, 2H), 8.24 (s, 1H). ^{13}C NMR (DMSO-d_6, 100.6 MHz): δ 32.6, 42.0, 43.1, 103.1, 110.1, 117.7, 119.2, 119.8, 121.7, 121.9, 124.3, 124.8, 126.1, 133.8, 135.6, 136.3, 136.5, 151.4, 156.9, 161.5, 170.6, 170.9. IR (KBr) ν_{max} 2941, 1703, 1544, 1331, 1226, 1121, 748 cm^{-1}.

AUTHOR INFORMATION

Corresponding Author

*For J.W.: phone, +41.61.696.23.85; fax, +41.61.696.24.55; e-mail, juergen.wagner@novartis.com. For P.v.M.: phone, +41.61.324.97.13; fax, +41.61.324.61.21; e-mail, peter.von_matt@novartis.com.

ACKNOWLEDGMENT

We thank Volker Brinkmann for the MLR studies and Karen Beltz for the solubility studies in simulated gastric fluids.

ABBREVIATIONS USED

SAR, structure−activity relationship; PKC, protein kinase C; CsA, cyclosporine A; DAG, diacylglycerol; PS, phosphatidylserine; TCR, T cell receptor; MLR, mixed lymphocyte reaction; log P, octanol/water partition coefficient; Pgp, P-glycoprotein; FaSSIF, fasted state simulated intestinal fluid; FeSSIF, fed state simulated intestinal fluid; MDCK, Madin−Darby canine kidney cell line; Caco-2, human colon carcinoma epithelial cell line

REFERENCES

(1) Dumont, F. J. Immunosuppressive strategies for prevention of transplant rejection. *Expert Opin. Ther. Pat.* **2001**, *11*, 377–404.

(2) Halloran, P. F. Immunosuppressive drugs for kidney transplantation. *N. Engl. J. Med.* **2004**, *351*, 2715–2729.

(3) Liu, E. H.; Siegel, R. M.; Harlan, D. M.; O'Shea, J. J. T cell-directed therapies: lessons learned and future prospects. *Nat. Immunol.* **2007**, *8*, 25–30.

(4) Wagner, J.; von Matt, P.; Sedrani, R.; Albert, R.; Cooke, N.; Ehrhardt, C.; Geiser, M.; Rummel, G.; Stark, W.; Strauss, A.; Cowan-Jacob, S. W.; Beerli, C.; Weckbecker, G.; Evenou, J.-P.; Zenke, G.; Cottens, S. Discovery of 3-(1*H*-indol-3-yl)-4-[2-(4-methylpiperazin-1-yl)quinazolin-4-yl]-pyrrole-2,5-dione (AEB071), a potent and selective inhibitor of protein kinase C isotypes. *J. Med. Chem.* **2009**, *52*, 6193–6196.

(5) Evenou, J.-P.; Wagner, J.; Zenke, G.; Brinkmann, V.; Wagner, K.; Kovarik, J.; Welzenbach, K. A.; Weitz-Schmidt, G.; Guntermann, C.; Towbin, H.; Cottens, S.; Kaminski, S.; Letschka, T.; Lutz-Nicoladoni, C.; Gruber, T.; Hermann-Kleiter, N.; Thuille, N.; Baier, G. The potent protein kinase C selective inhibitor AEB071 (sotrastaurin) represents a new class of immunosuppressive agents affecting early T cell activation. *J. Pharmacol. Exp. Ther.* **2009**, *330*, 792–801.

(6) Skvara, H.; Dawid, M.; Kleyn, E.; Wolff, B.; Meingassner, J. G.; Knight, H.; Dumortier, T.; Kopp, T.; Fallahi, N.; Stary, G.; Burkhart, C.; Grenet, O.; Wagner, J.; Hijazi, Y.; Morris, R. M.; McGeown, C.; Rordorf, C.; Griffiths, C. E. M.; Stingl, G.; Jung, T. The PKC inhibitor AEB071 may be a therapeutic option for psiorasis. *J. Clin. Invest.* **2008**, *118*, 3151–3159.

(7) Budde, K.; Sommerer, C.; Becker, T.; Asderakis, A.; Pietruck, F.; Grinyo, J. M.; Rigotti, P.; Dantal, J.; Ng, J.; Barten, M. J.; Weber, M. Sotrastaurin, a novel small molecule inhibiting protein kinase C: first clinical results in renal-transplant recipients. *Am. J. Transpl.* **2010**, *10*, 571–581.

(8) Newton, A. C. Regulation of the ABC kinases by phosphorylation: protein kinase C as a paradigm. *Biochem. J.* **2003**, *370*, 361–371.

(9) Tan, S.-L.; Parker, P. J. Emerging and diverse roles of protein kinase C in immune cell signalling. *Biochem. J.* **2003**, *376*, 545–552.

(10) Baier, G. The PKC gene module: molecular biosystematics to resolve its T cell function. *Immunol. Rev.* **2003**, *192*, 64–79.

(11) Guo, B.; Su, T. T.; Rawlings, D. J. Protein kinase C family functions in B-cell activation. *Curr. Opin. Immunol.* **2004**, *16*, 367–373.

(12) Ife, R. J.; Brown, T. H.; Blurton, P.; Keeling, D. J.; Leach, C. A.; Meeson, M. L.; Parsons, M. E.; Theobald, C. J. Reversible inhibitors of the gastric (H^+/K^+)-ATPase. 5. Substituted 2,4-diaminoquinazolines and thienopyrimidines. *J. Med. Chem.* **1995**, *38*, 2763–2773.

(13) Faul, M. M.; Winneroski, L. L.; Krumrich, C. A. A new, efficient method for the synthesis of bisindolylmaleimides. *J. Org. Chem.* **1998**, *63*, 6053–6058.

(14) Kosugi, M.; Negishi, Y.; Kameyama, M.; Migita, T. Palladium-catalyzed displacement of aryl halide by tin analogue of Reformatsky reagent. *Bull. Chem. Soc. Jpn.* **1985**, *58*, 3383–3384.

(15) Wolfe, J. P.; Buchwald, S. L. Palladium-catalyzed amination of aryl triflates. *J. Org. Chem.* **1997**, *62*, 1264–1267.

(16) Jagdmann, G. E.; Munson, H. R.; Gero, T. W. A mild efficient procedure for the conversion of carboxylic acid esters to primary amides using formamide/methanolic sodium methoxide. *Synth. Commun.* **1990**, *20*, 1203–1208.

(17) McCort, G.; Hoornaert, C.; Aletru, M.; Denys, C.; Duclos, O.; Cadilhac, C.; Guilpain, E.; Dellac, G.; Janiak, P.; Galzin, A.-M.; Delahaye, M.; Guilbert, F.; O'Connor, S. Synthesis and SAR of 3- and 4-substituted quinolin-2-ones: discovery of mixed 5-HT_{1B}/5-HT_{2A} receptor antagonists. *Bioorg. Med. Chem.* **2001**, *9*, 2129–2137.

(18) Kovarik, J. M.; Huang, H.-L. A.; Slade, A.; Sfikas, N.; Chandler, P. A. The effect on sotrastaurin pharmacokinetics of strong CYP3A inhibition by ketoconazole. *Br. J. Clin. Pharmacol.* **2009**, *68*, 381–385.

(19) Choc, M. G.; Mueller, E. A.; Robinson, W. T.; Kuhmle, A.; Smith, H. T.; Charnick, S. B. Relative bioavailability of Neoral versus Sandimmun in the presence of a P450IIIA and P-glycoprotein inhibitor. *Transplant Proc.* **1998**, *30*, 1664–1665.

(20) Weckbecker, G.; Pally, C.; Beerli, C.; Burkhart, C.; Wieczorek, G.; Metzler, B.; Morris, R. E.; Wagner, J.; Bruns, C. Effects of the novel protein kinase C inhibitor AEB071 (sotrastaurin) on rat cardiac allograft survival using single agent treatment or combination therapy with cyclosporine, everolimus or FTY720. *Transpl. Int.* **2010**, *23*, 543–552.

(21) For experimental details, see the following: Suomalainen, P.; Johans, C.; Soederlund, T.; Kinnunen, P. K. J. Surface activity profiling of

drugs applied to the prediction of blood−brain barrier permeability. *J. Med. Chem.* **2004**, *47*, 1783–1788.

(22) Frenkel, Y. V.; Clark, A. D.; Das, K.; Wang, Y.-H.; Lewi, P. J.; Janssen, P. A. J.; Arnold, E. Concentration and pH dependent aggregation of hydrophobic drug molecules and relevance to oral bioavailability. *J. Med. Chem.* **2005**, *48*, 1974–1983.

(23) Porter, C. J. H.; William, N. Transport and absorption of drugs via the lymphatic system. *Adv. Drug Delivery Rev.* **2001**, *50*, 1–2.

(24) Wasan, K. M. The role of lymphatic transport in enhancing oral protein and peptide drug delivery. *Drug Dev. Ind. Pharm.* **2002**, *28*, 1047–1058.

(25) Smits, R. A.; de Esch, I. J. P.; Zuiderveld, O. P.; Broeker, J.; Sansuk, K.; Guaita, E.; Coruzzi, G.; Adami, M.; Haaksma, E.; Leurs, R. Discovery of quinazolines as histamine H_4 receptor inverse agonists using a scaffold hopping approach. *J. Med. Chem.* **2008**, *51*, 7855–7865.

(26) Dawson, M. I.; Ye, M.; Cao, X.; Farhana, L.; Hu, Q.-Y.; Zhao, Y.; Xu, L. P.; Kiselyuk, A.; Correa, R. G.; Yang, L.; Hou, T.; Reed, J. C.; Itkin-Ansar, P.; Levine, F.; Sanner, M. F.; Fontana, J. A.; Zhang, X.-K. Derivation of a retinoid X receptor scaffold from peroxisome proliferator-activated receptor γ ligand 1-di(1*H*-indol-3-yl)methyl-4-trifluoromethylbenzene. *ChemMedChem* **2009**, *4*, 1106–1119.

(27) Ilovich, O.; Billauer, H.; Dotan, S.; Mishani, E. Labeled 3-aryl-4-indolylmaleimide derivatives and their potential as angiogenic PET biomarkers. *Bioorg. Med. Chem.* **2010**, *18*, 612–620.